Volume 41, April 2013   ISSN 0195-6671

CRETACEOUS
RESEARCH

Palynofacies analysis and palynology of the Agua de la Mula Member (Agrio Formation) in a sequence stratigraphy framework, Lower Cretaceous, Neuquén Basin, Argentina

M.V. Guler [a,d,*], D.G. Lazo [b,d], P.J. Pazos [b,d], C.M. Borel [a,d], E.G. Ottone [b,d], R.V. Tyson [c], N. Cesaretti [a], M.B. Aguirre-Urreta [b,d]

[a] Departamento de Geología, Instituto Geológico del Sur, Universidad Nacional de Sur, San Juan 670, 8000 Bahía Blanca, Argentina
[b] Instituto de Estudios Andinos "Don Pablo Groeber", Departamento de Ciencias Geológicas, Facultad de Ciencias Exactas y Naturales, Universidad de Buenos Aires, Pabellón II, Ciudad Universitaria, 1428 Buenos Aires, Argentina
[c] Getech, Elmete Hall, Elmete Lane, Leeds LS8 2LJ, UK
[d] Consejo Nacional de Investigaciones Científicas y Técnicas, Av. Rivadavia 1917, C1033AAJ Buenos Aires, Argentina

ARTICLE INFO

ABSTRACT

Variations in the sedimentary organic matter were documented throughout the Agua de la Mula Member (late Hauterivian) of the Agrio Formation, at a combined section in the type area of the Agrio Formation; the base at Agrio del Medio and the middle to top at Bajada del Agrio. A main organic-rich interval was identified in the basal Agua de la Mula Member, dominated by marine-derived Amorphous Organic Matter (AOM), coinciding with the highest Total Organic Carbon (TOC) content, between 1.4 and 3.8 wt.%, suggesting dysoxic conditions. The rest of the Member is predominantly characterized by terrestrially-derived organic matter, mainly phytoclasts, with low TOC values, around 1% or lower, indicating predominantly oxic depositional settings. By integrating stacking pattern and shell beds analysis, four depositional sequences SQ1–SQ4 were recognized. The organic-rich, finely laminated bituminous black shales of the *Spitidiscus riccardii* zone constitute a mayor and rapid inundation defining a Transgressive System tract (TST), related to a third order asymmetrical mesosequence dominated by a thick High System Tract (HST). It represents the most widespread and important flooding episode within the Neuquén Basin during the late Hauterivian. Inside sequences of higher frequency (SQ1, SQ2, SQ3, SQ4) of probably fourth order were recognized and analysed including several ammonids zones (*Spitidiscus riccardii*, *Crioceratites schlagintweiti*, *C. diamantensis* and *Paraspiticeras groeberi*). With the exception of the oxygen-controlled, basinal and outer ramp settings indicated for the TST1, which is equivalent to the TST of a lower order sequence, and the lower TST2, respectively, the prevalence of well oxygenated, inner to middle ramp depositional environments, is suggested for the rest of the sedimentary succession and emphasized in HST of SQ2, SQ3 and SQ4. Thus, a shallowing-upward trend with improved oxygenation is recorded through the Agua de la Mula Member, reflected by decreasing TOC, AOM content and preservation state of the organic matter. Based on the whole rock fluorescence analysis of the two selected organic-rich intervals from the *Spitidiscus riccardii* and the lowermost *Crioceratites diamantensis* zones, the presence of hydrocarbons suggests a very early *in situ* generation.

© 2012 Elsevier Ltd. All rights reserved.

1. Introduction

The marine bituminous black shales of the Agrio Formation constitute the source rocks of one of the most important Mesozoic oil systems of the Neuquén Basin (Cruz et al., 1996; 1998; Uliana et al., 1999; Tyson et al., 2005). Numerous studies have focused on the characterization of the organic matter and the depositional environments of these sedimentary rocks (e.g. Uliana and Legarreta, 1993; Cruz et al., 1996, 1998; Uliana et al., 1999). Tyson et al. (2005) used a combination of geochemistry and paly-nofacies to identify the presence of two organic-rich intervals, one at the base of the Pilmatué Member (Valanginian) and the other at the base of the Agua de la Mula Member (late Hauterivian), based upon five relatively distal outcrops of the Agrio Formation forming a north-south transect in the vicinity of the Chos Malal area. They

* Corresponding author. INGEOSUR, Universidad Nacional del Sur, San Juan 670, 8000 Bahia Blanca, Argentina. Tel.: +54 291 4595101x3064; fax: +54 291 4595148.
E-mail address: vguler@criba.edu.ar (M.V. Guler).

inferred a prevalence of dysoxic conditions towards the northern (distal) end of this transect. Spalletti et al. (2001) previously indicated predominantly anoxic basinal deposits in the Loma La Torre area close to the northern end of this transect.

The aim of the present work is to document and interpret qualitative and quantitative variations in sedimentary organic matter assemblages recovered from a relatively proximal section of the Agua de la Mula Member of the Agrio Formation exposed at Agrio del Medio and Bajada del Agrio (type locality of the unit). A precise ammonoid zonation established by Aguirre-Urreta et al. (2005, 2007) was utilized to correlate these two localities which encompass the *Spitidiscus riccardii*, *Crioceratites schlagintweiti*, *C. diamantensis*, and *Paraspiticeras groeberi* Zones of late Hauterivian-earliest Barremian age. Based on palynofacies, Total Organic Carbon (TOC) values, composition of palynomorph assemblage and macrofaunal analysis the changes in palaeoenvironmental conditions within a sequence stratigraphy framework are discussed in this paper.

2. Geological setting

The Neuquén Basin is located near the present international Argentine–Chilean boundary, between 32° and 40° S. The basin covers an area over 120,000 km^2 being represented by a narrow belt with a trend parallel to the present Principal Cordillera, mainly in Mendoza province, whereas in Neuquén province the basin expands to the east to form the Neuquén Embayment (Howell et al., 2005; Fig. 1). During Early Jurassic to Cretaceous times the basin was a retro-arc depocentre developed under active convergence of the western margin of South America. A well-developed volcanic arc was coeval with deposition under a rather constant thermal subsidence regime (Ramos and Folguera, 2005). Palaeoceanographic

marine connection was towards the Pacific Ocean, and the bulk of the clastic supply was from the southeast (Legarreta and Uliana, 1991).

The Agrio Formation was defined by Weaver (1931) in the Río Agrio section of central Neuquén. In the type locality the section reaches around 1,178 m, where its three members are very well-developed. The lower or Pilmatué Member is a marine succession mainly composed of massive clay shales, interbedded with thin layers of packstones and wackestones. Towards the top of the lower member the clay shales become dominant. The middle or Avilé Member is represented by yellowish brown, often cross-bedded sandstones of continental origin, lacking marine fossils. The upper or Agua de la Mula Member is a marine succession composed largely of massive clay shales in the lower part and grey calcareous shales interbedded with limestones and sandstones in the upper part (Leanza and Hugo, 2001). The marine members have a rich and abundant fossil record composed mainly of mollusks, corals and serpulids. Shell beds are a conspicuous component of the succession, and most of them are dominated by bivalves. Studies on ammonoids combined with nannoplankton and palynomorphs have provided an excellent biostratigraphy for the Agrio Formation (Aguirre-Urreta et al., 2005, 2007). The age of the unit ranges from late early Valanginian to earliest Barremian, although it varies according to position within the basin.

An open marine ramp depositional system subjected to storm influence has been inferred for the Agua de Mula Member at the Agua de la Mula locality and adjacent areas (Lazo et al., 2005). Further north, in Loma La Torre section, Spalletti et al. (2001) defined the predominance of basinal to outer ramp deposits deposited under suboxic to anoxic conditions, with subordinate shallower mid to inner ramp facies. Previous taphonomic and palaeoecologic studies have demonstrated that deposits of the
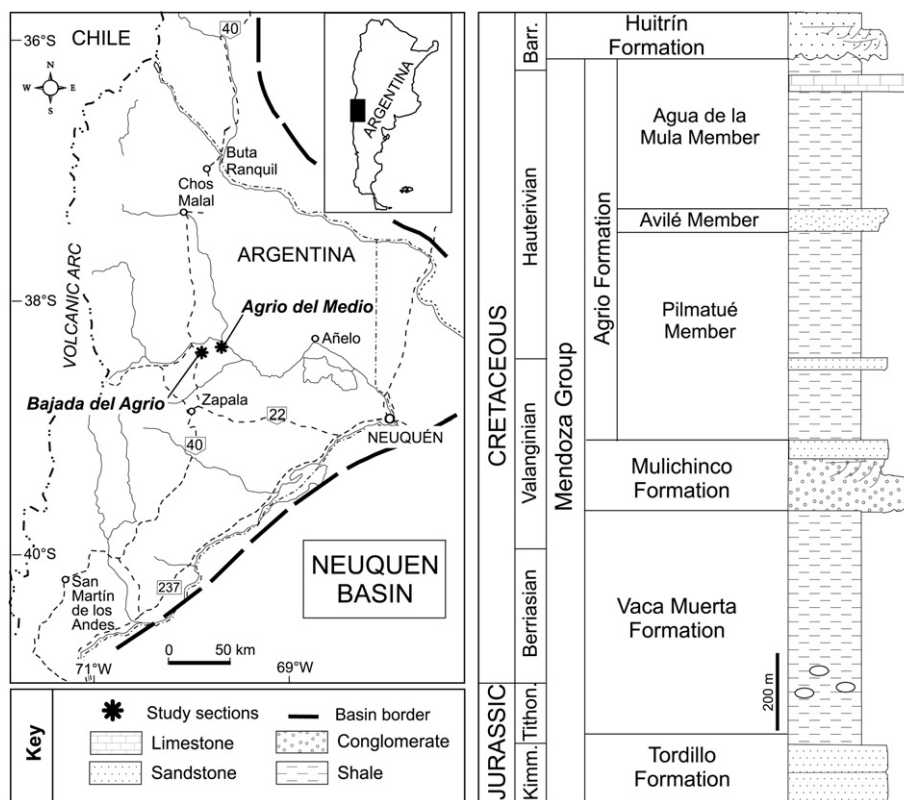

Fig. 1. Location map and lithostratigraphy of the Mendoza Group including the Agrio Formation, Neuquén Basin, west-central Argentina.

Agrio Formation in the Bajada del Agrio area record a diverse benthic macrofauna recorded in complex amalgamated shell beds. This is presumably related to its more proximal position within the basin, which Lazo (2007) has shown to be associated with a lower net sedimentation rate, higher abundance of amalgamation surfaces and a higher terrigenous input (Lazo, 2007). Lazo (2006) inferred a rather shallow marine ramp setting with alternating nearshore and proximal offshore deposits.

3. Materials and methods

3.1. Field logging, sampling and facies definition

A bed-by-bed analysis of the Agua de la Mula Member was performed combining two sections, Agrio del Medio (base, abbreviation: AM) and Bajada del Agrio (middle to top, abbreviation: AG), in the type area of the Agrio Formation (Weaver, 1931). The Agua de la Mula Member shows quite continuous outcrops on the western flank of the Río Agrio anticline, on the old track of the national road 40 (38° 25′S, 70° 00′W), with the exception of the basal levels of the *Spitidiscus riccardii* Zone (=*Spitidiscus* shales), and the contact with the Avilé Member, which are covered at Bajada del Agrio. The latter basal deposits can be recognized ca. 10 km northeast of Bajada del Agrio, at Agrio del Medio, where they are well exposed on the right margin of the Río Agrio (38° 20′S, 69° 57′W) (Fig. 1).

Lithofacies were defined on the basis of grain size, geometry, sedimentary structures, thickness and bed contacts. Several lithofacies have been identified: laminated dark bluish shales and marls, laminated dark grey shales, grey fine to medium sandstones, dark grey oolitic and bioclastic limestones and heterolithic bedding (lenticular to wavy). A detailed description of similar lithofacies can be found in Lazo et al. (2005).

The macrofaunal content of the rocks was described taking into account stratigraphic, taphonomic and palaeontological qualitative observations, and with an emphasis on the shell beds. The following variables were considered: shell packing, orientation, grading, geometry, fragmentation, corrosion, encrustation, and bioerosion. The diversity of taxa and range of life habits present in each concentration was also considered. Particular attention was paid to pavements of gryphaeid oysters, inoceramids or ammonoids which are interpreted as flooding events. Beds containing flat and globose coral colonies were also carefully described. Shell beds were classified according to their position within sequences in onlap/backlap and toplap concentrations following the approach of Banerjee and Kidwell (1991). Onlap/backlap concentrations are located at the bases of the sequences while toplap concentrations occur at the top. The sequences were defined taking into account several features like stacking pattern as the most important but also, diagnostic surfaces or intervals and paleobatimetric indicators as storm sedimentary structures (hummocky), wave ripples and fossil concentrations.

3.2. Organic matter analysis

Palynological samples were taken throughout the section from almost every shale bed exposed. The sample codes comprise a number corresponding to the sampled bed and a suffix letter that indicates the subsample within that bed. A total of 47 samples were processed for the palynological analysis; the basal 6 samples (AM0–4 and AM926) are from Agrio del Medio, and the other 41 samples from Bajada del Agrio. All samples were palynologically productive. The chemical processing included HCl and HF treatment for the removal of the inorganic components. Neither ultrasonic treatment nor oxidative methods were employed. Residues were first sieved at 10 and 20 μm and then mounted in glycerin jelly. For the quantitative analysis, more than 300 organic particles larger than 10 μm were counted per sample. Light microscopy was undertaken using a Nikon Eclipse 600 serial number 77255 and an attached Nikon Coolpix 950 digital camera. The figured palynological material illustrated in Figs. 8–11 is housed in the collection of the Departamento de Ciencias Geológicas, Universidad de Buenos Aires, Buenos Aires, Argentina.

The classification scheme and the description of the dispersed sedimentary organic matter components are summarized in Table 1. Four main categories were identified: (1) phytoclasts: black and dark brown translucent, equidimensional (equant) or lath-shaped, a few are biostructured and black opaque, equidimensional or lath-shaped; (2) terrigenous palynomorphs: spores and pollen grains; (3) marine palynomorphs: organic-walled dinoflagellate cysts, acritarchs, prasinophytes and foraminiferal linings; and (4) amorphous organic matter (AOM): granular-textured brown amorphous fragments; scarce orange gels are also present in some samples. Additionally, except when indicated with an asterisk (*), more than 200 palynomorphs were counted from the 20 μm sieved residue, in order to calculate the ratio of marine palynomorphs to terrestrial sporomorphs (the M/T ratio) or its inverse (T/M ratio). Frequencies of the dominant taxa groups of miospores were calculated from additional counts, whereas dinoflagellate cyst taxa were only quantified in assemblages with M/T ratios ≥0.5. The ratio of AOM to phytoclasts was also calculated.

Statistical analysis and visual observations were used to identify palynofacies groups. Relative frequencies of the main categories of sedimentary organic matter (Fig. 3), and of palynomorphs, dinoflagellate cysts and miospores taxa (Fig. 4), were calculated and represented using Tilia package (Grimm, 1991). Statistical analysis was performed using Statistica (version 9.1). Non-stratigraphically constrained cluster analysis was carried out on standardized ratios of sedimentary organic matter variables identified as showing the greatest information content, using squared Euclidean distance and Ward's minimum variance method. The AOM-rich samples at the base of the section were not incorporated in the cluster analysis as there were missing data for some of the variables. Ternary AOM-phytoclast-palynomorph ("APP") diagrams were prepared using Tridraw (version 4.5a) and show the varying percentages of the three components within each of the palynofacies groups (Fig. 7).

Total Organic Carbon (TOC) contents were determined from samples powdered in a mechanical mortar, decarbonated with HCl and analysed by LECO equipment at LANAIS N-15 CONICET-UNS (Departamento de Agrononomía, Universidad Nacional del Sur).

Water suspensions of palynological residues were examined under fluorescence to evaluate the preservation of the organic matter. Samples with higher TOC values and higher percentages of AOM from the AG3a–d and AM0–4 intervals were selected to analyse the colour and intensity of fluorescence on slides of the whole rock, in order to assess the maturity of the organic matter (Riecker, 1962). Whole rock auto fluorescence was analysed on uncovered double polished thin sections of the rocks, prepared at the Laboratorio de Petrotomia (Departamento de Geología, Universidad Nacional del Sur). The fluorescence observations were made with an Olympus BH2-RFC (Reflected Light Fluorescence Attachment) microscope, using blue incident light (wavelengths 435 nm and spectrum regions near 490 nm) and yellow filter (wavelengths 570–590 nm).

4. Sequence stratigraphic framework

Legarreta and Gulisano (1989) published a first attempt to analyse the sedimentary record of the Neuquén Basin using

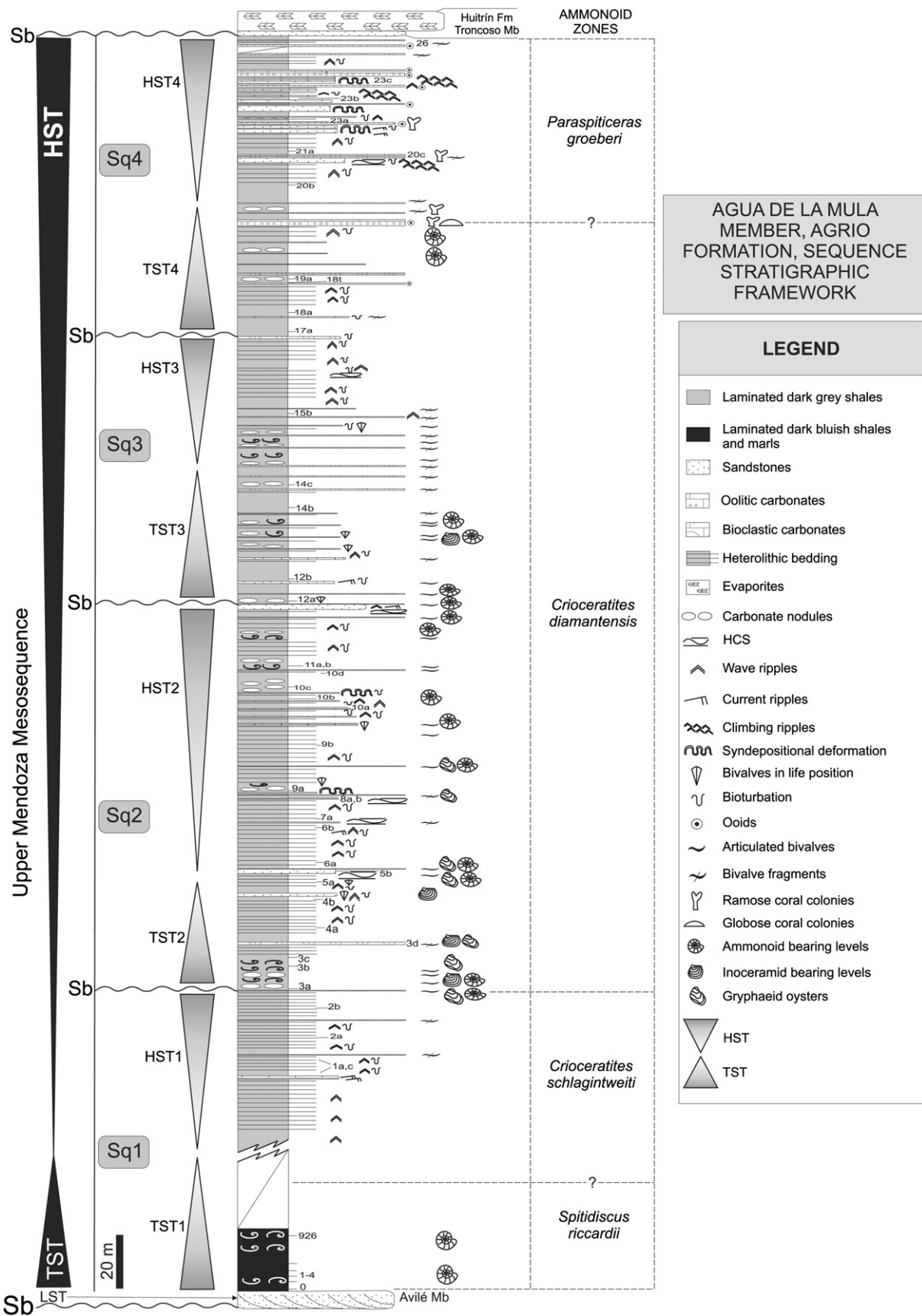**Fig. 2.** Lithological log and sequence stratigraphy of the Agua de la Mula Member, Agrio Formation at the Agrio del Medio and Bajada del Agrio localities, Neuquén Basin. The described succession is included in a third order sequence containing a TST and HST (dark grey) with a strongly asymmetrical stacking pattern. Sequences of higher order and lower frequency are recognized within the interval and analysed in this paper.
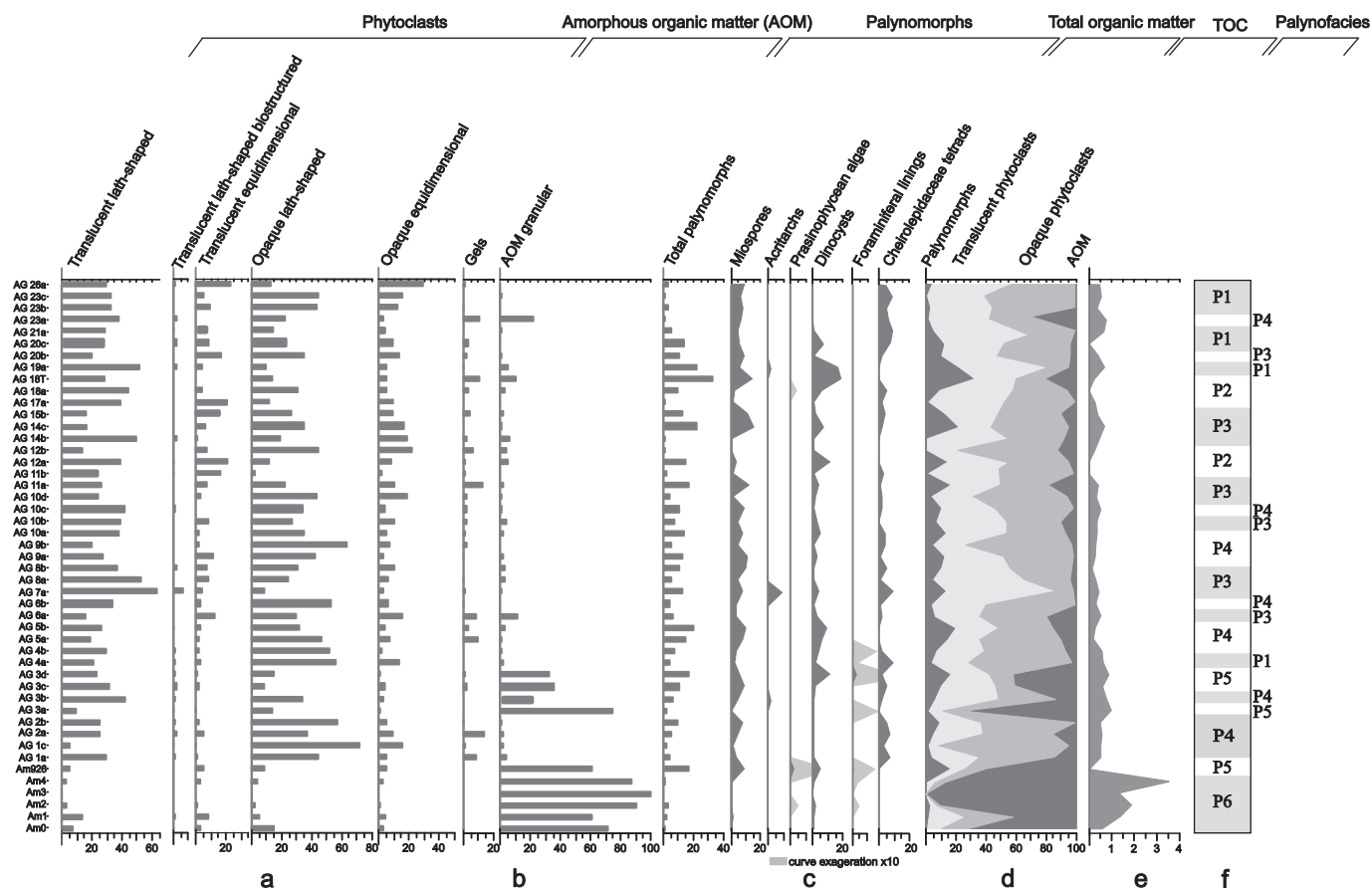
Fig. 3. Relative frequencies of selected sedimentary organic matter components, Total Organic Carbon (TOC) percentages and related palynofacies identified through the Agua de la Mula Member. Selected categories percentages over total organic matter are represented: A. lath-shaped, biostructured, equidimensional translucent phytoclasts and lath-shaped, equidimensional opaque phytoclasts; B. marine-derived AOM and gels of presumably terrestrial origin; C. total palynomorphs, miospores, acritarchs, prasinophytes, dinoflagellate cysts, foraminiferal linings and pollen tetrads; D. a striplog of the percentages of the main categories; E. graphic representation of the TOC percentages; F. palynofacies P1, P2, P3, P4, P5 and P6.

a sequence stratigraphy approach. They proposed three super-sequences encompassing the latest Triassic to Paleocene deposits. The Agrio Formation is included in their middle supersequence. In particular the Avilé and Agua de la Mula Members are included into the named "Upper Mendoza Mesosequence" which is within sub-divided into four depositional sequences. The "Upper Mendoza Mesosequence" and its internal divisions into four, higher order depositional sequences are depicted in Fig. 2, where is clearly visible that the TST of the mesosequence is equivalent in thickness to the TST1 of the SQ1.

Recently Archuby et al. (2011) also proposed a sequence strati-graphic framework for the Agua de la Mula Member that does not differ with the scheme proposed by Spalletti et al. (2001) for the north of the basin. However, in their scheme three basal siliciclastic sequences are overlain by a fourth carbonate-dominated sequence towards the top of the unit, which is dominated by tidal influenced deposits (Pazos et al., 2012). In the present study we also divide the Agua de la Mula Member into four depositional sequences mainly based on their stacking pattern (SQ1—4 in Fig. 2) with a noticeable absence of lowstand deposits (LST). The taphonomy and palae-oecology of shell beds were also taken into account in order to recognize periods of low net sedimentation rate such as omission, amalgamation and reworking. Each sequence is characterized by a basal transgressive (TST) followed by a highstand systems tract (HST).

4.1. The lowstand systems tract (LST) of the "Upper Mendoza Mesosequence" (Avilé Member)

This is the only well-recognized LST in the Agrio Formation. It entirely encompasses the deposits of the Avilé Member at the base of the logged section. This unit is very well known (hydrocarbon reservoir) and has been characterized as fluvial and aeolian deposits developed after a major relative sea level fall related to the "Upper Mendoza Mesosequence". The sea level fall almost completely desiccated the entire basin (Legarreta and Gulisano, 1989; Veiga et al., 2002). This sandstone package is intercalated between ammonoid-bearing marine deposits of the Pilmatué and Agua de la Mula Members and it is also interpreted as a forced regression (Veiga et al., 2002), but the amount of erosion involved in the incision at the base is unknown. However, the progradation of a fluvial wedge onto marine deposits was rapid, considering that none of the ammonoid zones of the Pilmatue Member are absent and a relative conformable disposition of the fluvial deposits suggests that most of the sediments were bypassed without deep incision during the sea level drop.

At Bajada del Agrio locality, the Avilé Member is around 10 m in thickness and is composed of medium to coarse-grained sand-stones with trough cross-stratification indicating palaeoflows towards the NW. It has an erosive basal contact with the dark grey shales of the Pilmatué Member and contains abundant intrabasinal
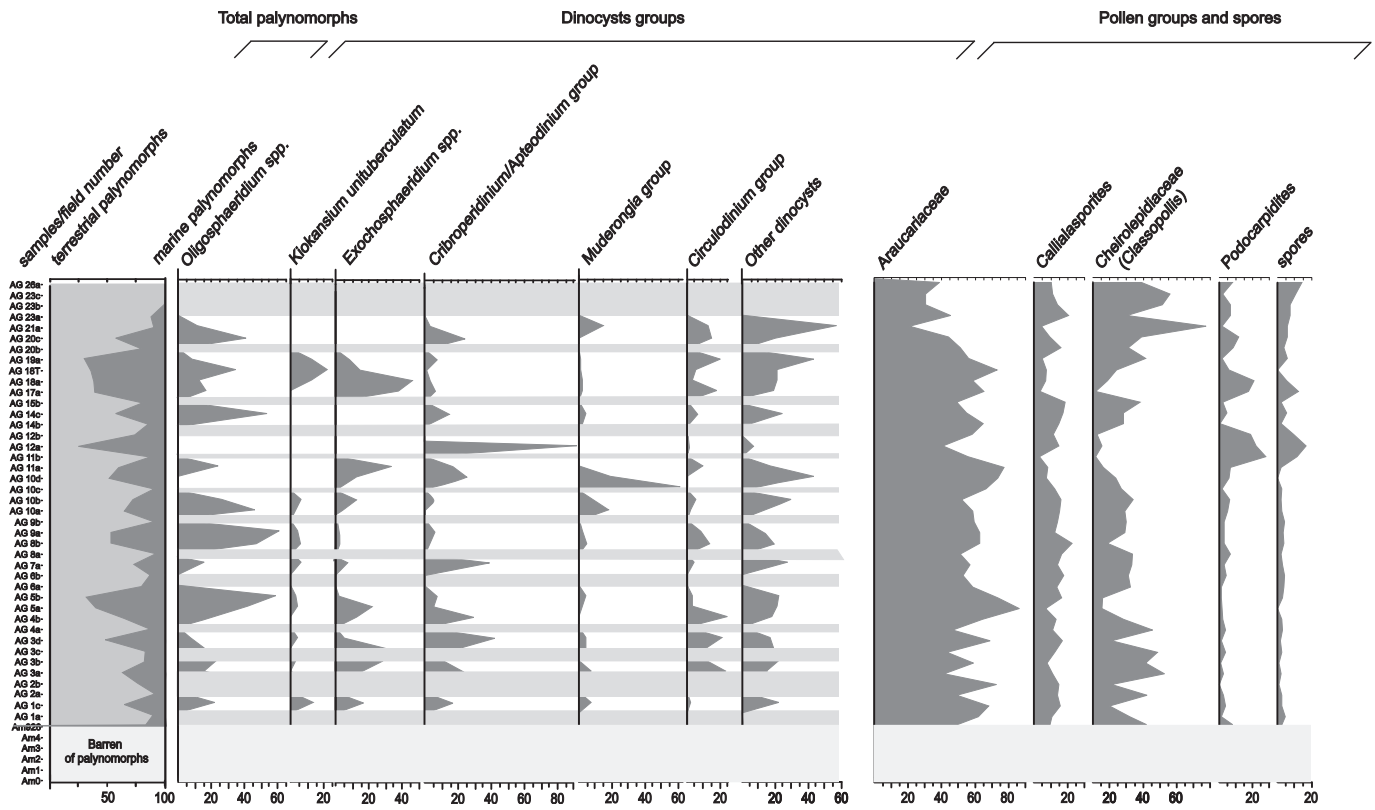
Fig. 4. Diagram of continental vs marine palynomorphs and relative frequencies of selected dinoflagellate cysts and miospores groups through the Agua de la Mula Member. Frequencies of dinoflagellate cyst taxa were calculated as a percentage of total dinoflagellate cysts and are represented only in the intervals with the highest M/T ratios ("dinoflagellate cyst peaks"), grey bands indicate number of dinoflagellate cysts less than 150. Frequency of miospore taxa was calculated as a percentage of total miospores. In the AM1–AM4 interval palynomorphs are extremely scarce or probably masked by AOM.

clay-chips eroded from the underlying member and define the sequence boundary of the "Upper Mendoza Mesosequence". The Avilé Member is sharply overlain by black and dark-bluish shales and marls of the Agua de la Mula Member. Synsedimentary deformation observed close to the contact of both members and the lack of transitional facies or shoreface deposits suggest an accretionary transgression (*sensu* Helland-Hansen and Martinsen, 1996) resulting from a rapid relative rise in sea level.

4.2. Characterization of transgressive systems tracts (TSTs)

The TST1 located in the *Spitidiscus riccardii* zone at the base of the section is particularly interesting as it is composed by 20 m of finely laminated bituminous black and dark-bluish shales and marls ("paper shales"). These deposits record a regional transgressive episode that seals the potential reservoir facies of the Avilé Member.
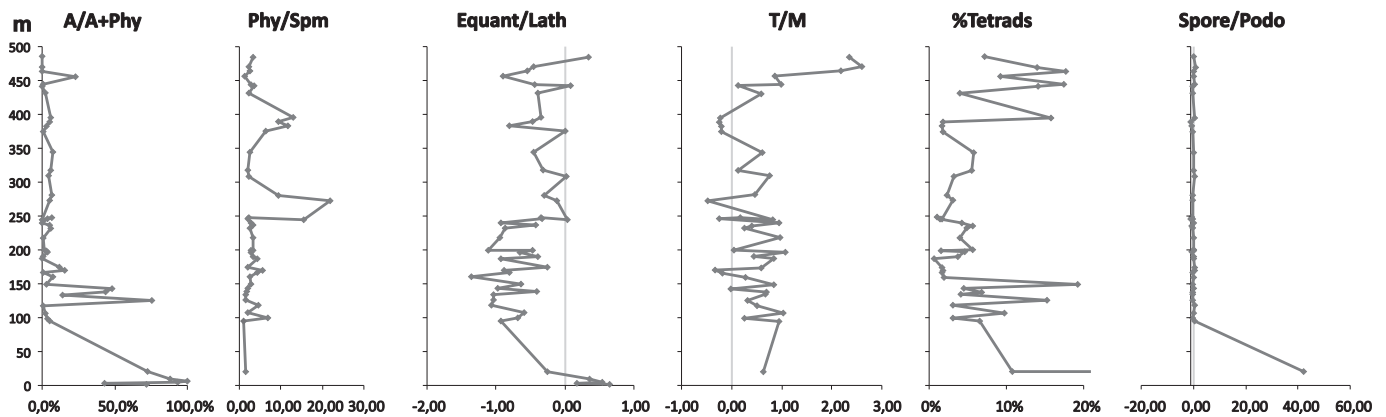
Fig. 5. Stratigraphical trends in six parameters through the Agua del la Mula Member, mostly ratios of sedimentary organic matter variables. The parameters were used for the clustering analysis: A/A+Phy, Phy/Spm, Equant/Lath, T/M, %Tetrads and Spore/Podo. A = amorphous organic matter, Phy = phytoclasts, Spm = sporomorphs, Equant = opaque equidimensional phytoclasts, Lath = opaque lath phytoclasts, T = terrestrial palynomorphs, M = marine palynomorphs, Tetrads = tetrads of Classopollis, Podo = pollen of Podocarpaceae, m = metres.
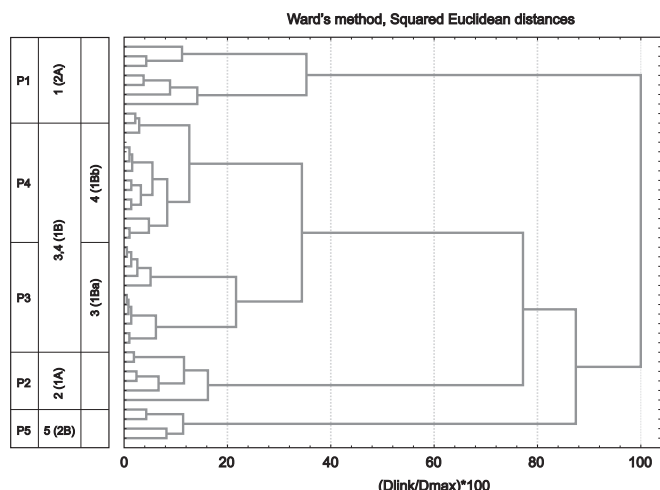
Fig. 6. Dendrogram generated by non-stratigraphically constrained squared Euclidean distance and Ward's minimum variance method cluster analysis, in samples from the post "*Spitidiscus* shales" interval. It shows four groups of samples designed palynofacies 1–5, from the most proximal to the most distal.

The benthic macrofauna of the *Spitidiscus* shales is scarce and recorded in discrete levels of dispersed shells. They are composed of small-sized bivalves and gastropods (L < 2–5 cm). The bivalves include a relatively low diversity assemblage of small arcoids and heterodonts while the gastropods include only one species of aporrhaid. Low degrees of corrosion, disarticulation, fragmentation, incrustation and bioerosion point to a quiet environment and indicate that lateral transport of shells was insignificant. The overall small size of the benthic elements is suggestive of a reduced oxygen level at the sediment-water interface. Ammonoid body chambers and crushed phragmocones and external moulds are quite frequent in this interval.

The post-*Spitidiscus* TST intervals are characterized by basal transgressive shell beds (onlap/backlap concentrations). The sharp to erosive basal contact of these shells beds correspond to sequence boundaries of each of the three studied depositional sequences. Shell beds may be simple and thin (less than 0.5 m) or complex/amalgamated and thick (up to 2 m). They have loose to dense shell packing and include variably preserved fossils with preferably parallel orientation. Background shell debris and whole valves are

Fig. 7. Ternary APP diagram (*sensu* Tyson, 1995) showing the varying proportions of amorphous organic matter, palynomorphs and phytoclasts in the six palynofacies. Palynofacies 1–4 were grouped due to they are not clearly differentiated in terms of APP data.

usually mixed. Shells record variable taphonomic modifications. Shell beds are composed by winnowed bivalves, gastropods, nautilids, and ammonoids. In particular TST4 is characterized by abundant oolitic and bioclastic limestone deposits including levels with frequent flat globose and ramose coral colonies. Most of these basal shell beds are interpreted as onlap/backlap levels and thus include the maximum flooding interval in each depositional sequence, except perhaps in SQ2 (see below).

The basal shell beds are overlain by laminated dark grey shales containing abundant levels of cm-sized calcareous nodules. The nodules occasionally show borings or small encrusting oysters. Fine bioturbation and concretionary *Thalassinoides* sp. also occur. Ammonoids are frequently recorded uncrushed in nodules. Thin shell pavements of gryphaeid oysters and inoceramids are frequently intercalated, especially within interval AG3a–d. They show low degrees of taphonomic alteration as they are mostly articulated and lack bioerosion or incrustation, pointing to a quiet environment where shells were winnowed *in situ* (backlap/maximum flooding interval).

4.3. Characterization of highstand systems tracts (HSTs)

The HSTs are characterized by alternating olive grey shales and yellowish fine to medium-grained sandstones with different heterolithic (lenticular, wavy, and flaser bedding) deposits but also with cross-stratification with oscillatory or combined-flow features. The general stacking pattern is coarsening, shallowing and thickening-upward. In the siliciclastic sandstone beds lags of reworked nodules, crudely graded bedding of matrix or bioclasts, valve stacking, massive or plane lamination, hummocky cross-stratification, ripple cross-lamination, and wave ripples were all documented. The top of most of these beds exhibits a diverse trace fossil assemblage belonging to the *Cruziana* ichnofacies.

Occasionally these facies are topped by amalgamated sandstones bodies up to 5 m in thickness that shows moderate to high degrees of bioturbation. Shell beds with siliciclastic silty matrix are usually intercalated with these bodies (toplap concentrations). They are characterized by disperse to loose shell packing, high articulation and low degrees of corrosion, fragmentation, incrustation and bioerosion. Semi-infaunal and infaunal bivalves usually occur in life position. Ammonoids may be abundant and parallel to bedding on the top of the sandstone beds.

5. Palynology

5.1. Palynofacies analysis

Marine-derived AOM, phytoclasts, terrestrial and marine palynomorphs constitute the four main components of the dispersed organic matter analysed through the Agua de la Mula Member. The categories and subcategories identified are listed in Table 1 and their relative frequencies plotted in Fig. 3. High proportions of marine-derived AOM characterize the *Spitidiscus riccardii* Zone shales, whereas most other organic matter components are absent. Consequently, the AOM-rich samples at the base of the section were not incorporated in the cluster analysis, but have been designated arbitrarily as "pseudocluster" 6. These samples have the highest content of marine –derived AOM, with percentages that exceed 60% and correlate with the highest TOC values (between 1.4 and 3.8 wt.%). A non-stratigraphically constrained cluster analysis on the organic matter count data was performed on the post *S. riccardii* zone samples interval, which allowed the identification of four main groups of samples (clusters 1A, 1B, 2A, and 2B). In turn, cluster 1B is divided in subclusters 1Ba and 1Bb (Fig. 6). Stratigraphic
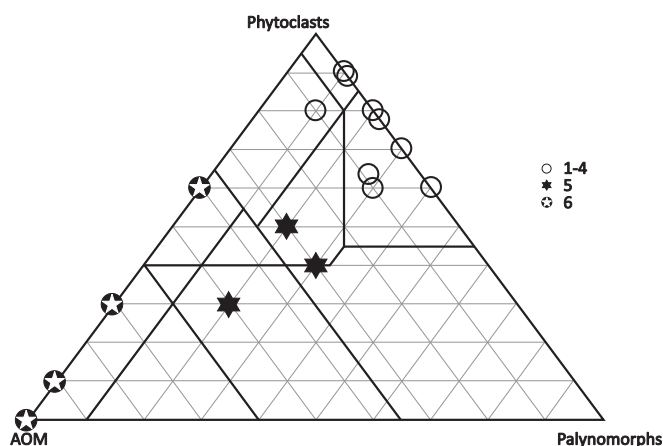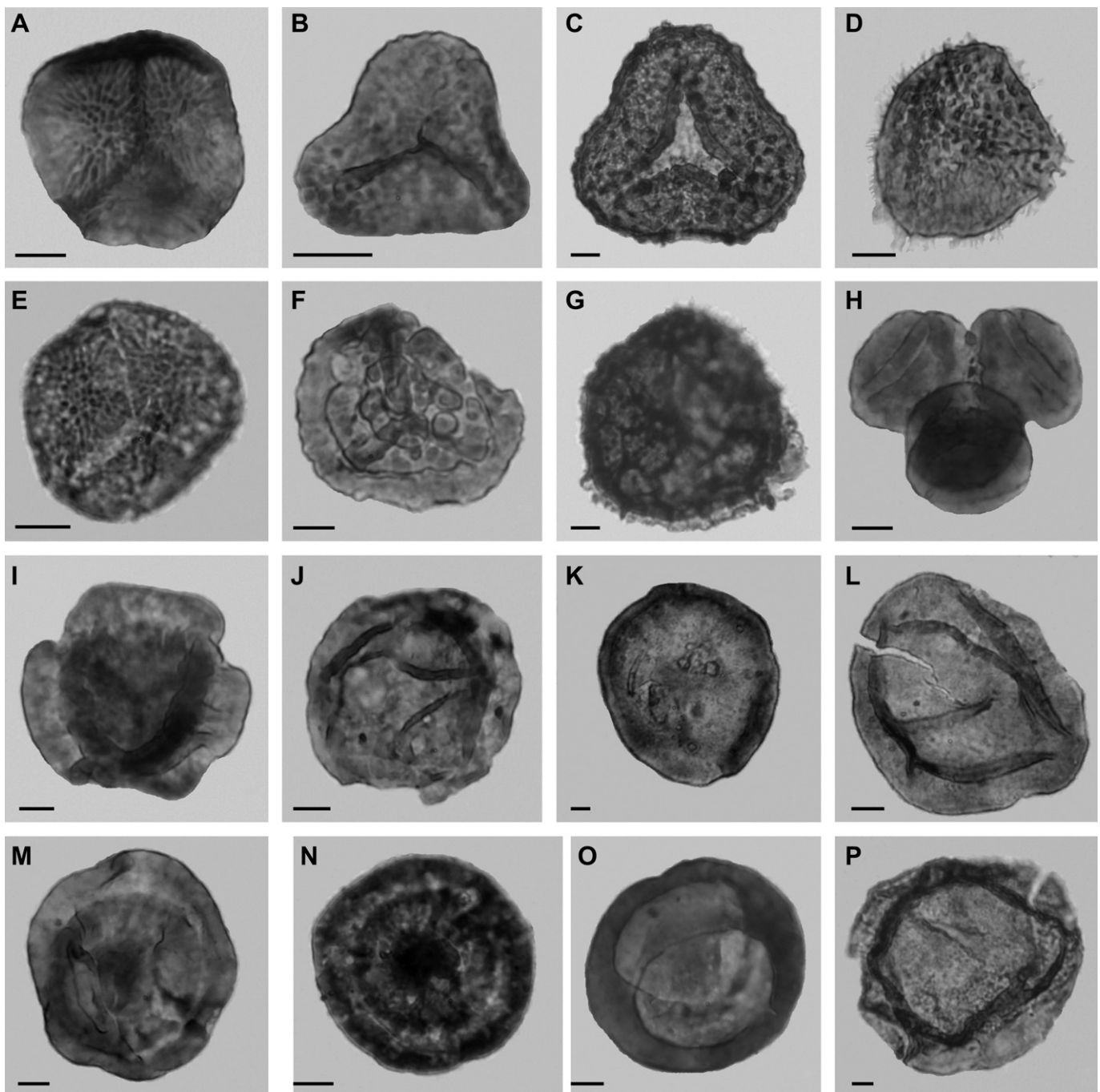
Fig. 8. Pollen grains and spores identified in the Agua de la Mula Member. A, E, *Nevesisporites radiatus* (Chlonova) Srivastava 1972; A, BAFC-Pl 2136(1) Y22/2; E, BAFC-Pl 2139(2) T28/2. B, *Concavissimisporites* sp., BAFC-Pl 2147(1) G47/2. C. *Concavissimisporites* sp., BAFC-Pl 2133(1) A43/1. D, *Ceratosporites* sp., BAFC-Pl 2170(1) L33/0. F, *Interulobites intraverrucatus* Phillips in Phillips and Felix 1971, BAFC-Pl 2148(1) T20/4. G, *Retitriletes* sp., BAFC-Pl 2141(1) N47/0. H, *Classopollis* sp., BAFC-Pl 2133(1) Y37/2. I, *Callialasporites trilobatus* (Balme) Dev, BAFC-Pl 2147(1) R21/3. J, *Callialasporites turbatus* (Balme) Schulz, BAFC-Pl 2139(1) O30/0. K, *Balmeiopsis limbatus* (Balme) Archangelsky, BAFC-Pl 2166(1) P42/1. L, *Araucariacites australis* Cookson, BAFC-Pl 2140(1) G9/2. M, *Cyclusphaera radiata* Archangelsky in Archangelsky et al., BAFC-Pl 2133 K54/3. N, *Cyclusphaera radiata* Archangelsky in Archangelsky et al., BAFC-Pl 2129(1) W48/0. O, *Cyclusphaera psilata* Volkheimer and Sepúlveda, BAFC-Pl 2133(1) W45/3. P, *Araucariacites australis* Cookson, BAFC-Pl 2136(1) Y25/2. Scale bar: 10 μm

variation of the key parameters used in the clustering are plotted in Fig. 5, mostly expressed as ratios or log ratios. The clusters were "profiled" by ranking the mean values of the selected parameters. The average rank scores were then used to renumber the clusters such that cluster 1 (2A) represented the most proximal palynofacies characteristics and cluster 5 (2B) the most distal, based on the typical patterns usually exhibited by these parameters. The intermediate cluster 2 (1A) and subclusters 3

(1Ba) and 4 (1Bb) are progressively more proximal in character. As some of the parameters do not express their classic proximal–distal relationships in this dataset, the renumbering was also designed to produce the most coherent overall stratigraphic order of clusters.

In cluster 5, the content of AOM is relatively high, ranging from 42 to 100% (mean 52%) and phytoclast percentages are less than 52%. These palynofacies characterize samples AG3a–3d from the
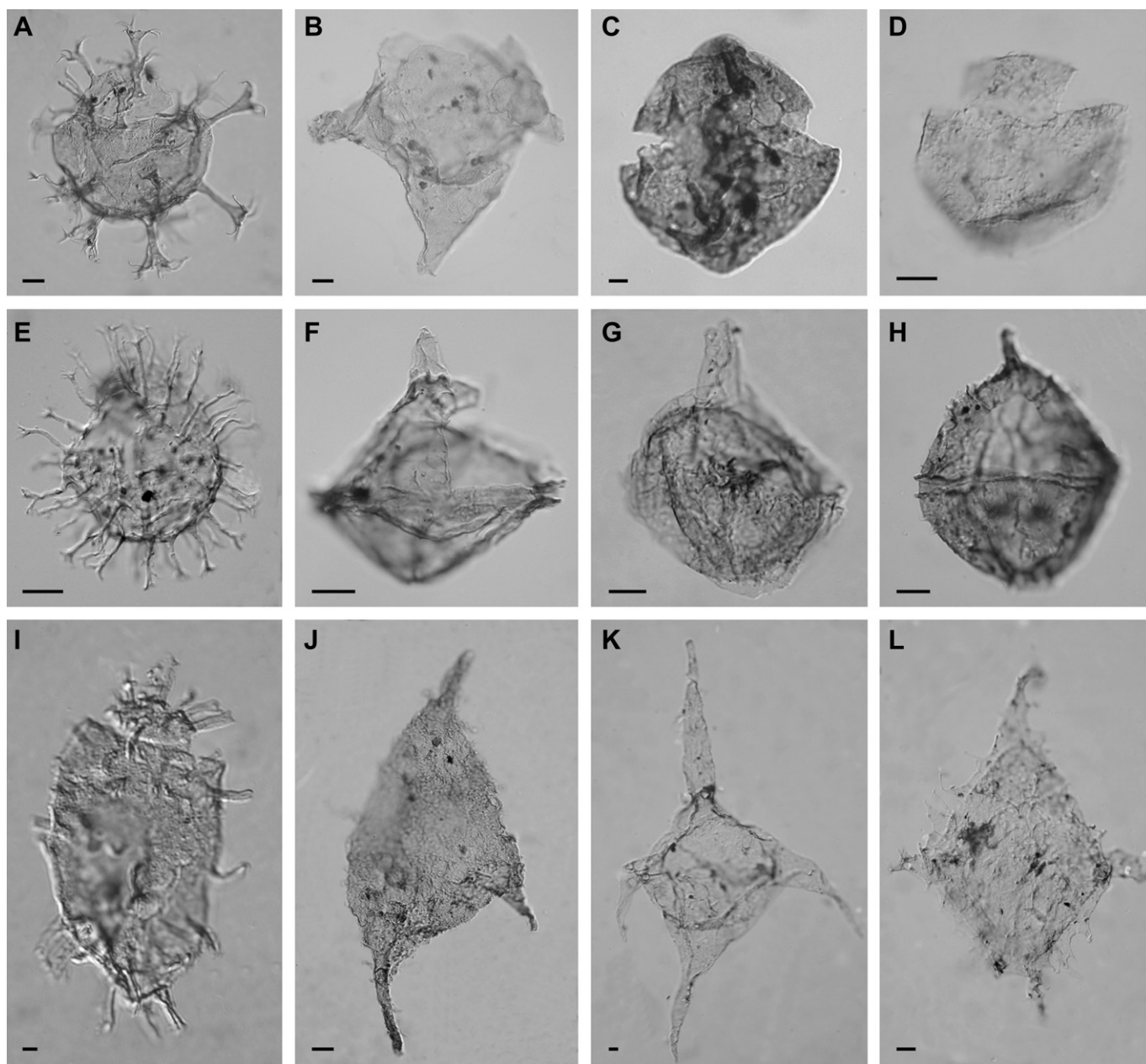
Fig. 9. Organic-walled dinoflagellate cysts recovered in the Agua de la Mula Member. A, *Oligosphaeridium complex* (White) Davey and Williams BAFC-PI AG1c/2812(2) W44/3; ventral view, high focus. B, *Muderongia* cf. *pariata* Duxbury BAFC-PI 2884(2) D47/4; ventral view, high focus. C, *Mendicodinium* sp. BAFC-Pl AG2a/2777 K44; ventral view, intermediate focus. D, *Kallosphaeridium* sp. BAFC-Pl AM926 L36; dorsal view, high focus. E, *Kiokansium unituberculatum* (Tasch in Tasch et al.) Stover and Evitt. BAFC-Pl AG14b/2780 R23/2; oblique lateral view, high focus. F, *Occisucysta tentoria* Duxbury *emend*. Jan du Chêne et al. AG14c/2881(2) S36/3 left lateral view, high focus. G, *Dingodinium cerviculum* Cookson and Eisenack *emend*. Khowaja-Ateequezzaman et al. BAFC-PI 2884 (2) Q39/4; left lateral view, high focus. H, *Cribroperidinium orthoceras.* (Eisenack) Davey BAFC-Pl AG3d/2785 A53; dorsal view, high focus. I, *Tanyosphaeridium magneticum* (Davies) Torricelli BAFC-Pl AG19a/2884 G40/3; dorsal view, high focus. J, *Pseudoceration pelliferum* (Gocht) Dörhöfer y Davies AG1a/2811 H53/2; dorsal view, high focus. K, *Muderongia brachialis* Ottone and Pérez Loinaze, BAFC-Pl AM926 O46/2; dorsal view, intermediate focus. L, *Phoberocysta neocomica* BAFC-Pl AM926 Q48/3; ventral view, intermediate focus. Scale bar: 10 μm

base of the *Crioceratites diamantensis* zone, associated with TOC values close to 1 wt.%. Marine palynomorph proportions are variable, between 20 and 60% of the total palynomorphs, and foraminiferal linings are best represented in these intervals, being absent in the rest of the section. Low spore/bisaccate ratios correlate with higher proportions of tetrads, ranging from 4.5 to 15.3%.

Palynofacies in cluster 1, 2 and subclusters 3 and 4 exhibit strong dominance of phytoclasts, with percentages of AOM less than 10% and associated TOC values less than 1 wt.%. These

clusters are very similar in APP terms (Fig. 7). Nevertheless, the palynofacies of cluster 1, which characterize the top of the section, have percentage values of phytoclasts between 67% and 100%, and the palynomorph assemblages record the highest proportions of sporomorphs (between 57% and 100 % of total palynomorphs), the highest percentages of *Classopollis* tetrads, (from 7% to 19%), and the highest spore/bisaccate ratio. The increase in tetrads in clusters 1 and 5, and their correlation with the other parameters, does not conform to a single unidirectional trend. In cluster 1, high tetrad values correlate with parameter of
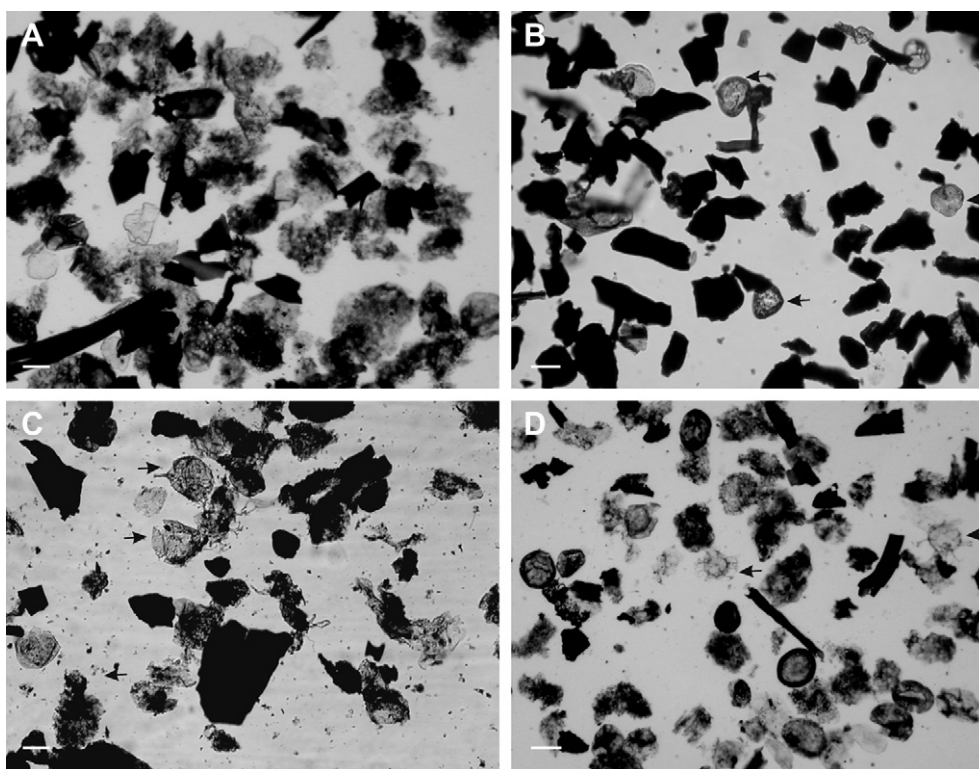
Fig. 10. Sedimentary organic matter from the Agua de la Mula Member. A, Palynofacies 2 from level AG3a, at the base of the *Crioceratites diamantensis* zone, highly dominated by marine-derived AOM. B, Phytoclast-dominated palynofacies 4 from level 23a, in the *Paraspiticeras groeberi* zone; pollen grains and spores (arrowed) are the main components of the palynomorph assemblage. C, Palynofacies 2 from level AG3d in the lower *Crioceratites diamantensis* zone, highly dominated by marine-derived AOM and dinoflagellate cysts; *Cribroperidinium* and *Circulodinium* taxa (arrowed) dominate the dinoflagellate cyst assemblage. D, Palynofacies 2 from level AM926 from the top of the *Spitidiscus riccardii* zone; highly dominated by AOM and dinoflagellate cysts, lower proportions of miospores and phytoclasts complete the assemblage. Scale bar: 50 μm

the most proximality, whereas in cluster 5 most of the other parameters indicate distal environmental conditions. This may be because the frequency of tetrads can reflect both supply and lower disarticulation in distal, low energy depositional settings (Tyson, 1995).

Cluster 2, and subclusters 3 and 4 embrace the approximately 200–400 m – interval in the middle part of the section, where T/M ratio fluctuates widely and tetrads reach the lowest values. The strong dominance of phytoclasts indicated by the highest Phy/Spm ratio characterize cluster 2. In a few samples of this cluster, marine palynomorphs outnumber terrestrial palynomorphs (with dinoflagellate cysts exceeding 60%), and thus the T/M ratio shows its lowest values, coinciding with the highest bisaccate proportions (lowest spore/bisaccate ratios; highest Podocarpaceae in Fig. 4). In the whole interval the different parameters do not show mutually consistent proximal–distal trends and their values commonly overlap. This could indicate that the degree of absolute proximal–distal variation in this interval is not sufficient to result in clear trends in the organic matter assemblages.

5.2. Terrestrial palynomorphs

The proportion of terrestrial components ranges from 25 to 100% of total palynomorphs and the different taxa identified throughout the Agua de la Mula Member are listed in Appendix A. Miospores are dominated by pollen of Araucariaceae, along with a consistent representation of Cheirolepidiaceae and Podocarpaceae. Bryophyte, Pteridophyte and Lycophyte spores are minor constituents.

Araucarian pollen grains such as *Araucariacites australis* Cookson, *Balmeiopsis limbatus* (Balme) Archangelsky, *Cyclusphaera psilata* Volkheimer and Sepúlveda and *C. radiata* Archangelsky in Archangelsky et al. (Archangelsky 1977, 1994; Baldoni, 1979; Del Fueyo, 1991; Dettmann and Jarzen, 2000; Del Fueyo and Archangelsky, 2005) make up about 9–35% of the total. Inaperturate forms that appear to be damaged Araucarian pollen grains (about 8–36%) are also well represented. *Callialasporites* comprises ca. 2–15% of the total. This morphogenus was referred to the Podocarpaceae (Gamerro, 1965; Archangelsky, 1966; Townrow, 1967) but also to the Araucariceae (van Konijnenburg-van Cittert, 1971). The araucariaceous origin of *Callialasporites* was proposed by Balme (1957, p. 32), and Batten and Dutta (1997, p. 49). *Classopollis*, the pollen of Cheirolepidiaceae (Balme, 1995), commonly represents about 2–46% of the total assemblage; however, it makes up 61% of the total in horizon AG21a, and is the dominant form towards the uppermost part of the section. Disaccate podocarpaceous pollen grains (Archangelsky and Villar de Seoane, 2005), comprise less than 6%. Spores occur quite sporadically (0–11%). Bryophyte spores include *Aequitriradites* sp., *Foraminisporis* spp., *Nevesisporites radiatus*, and probably, *Interulobites intraverrucatus* (Krutzsch, 1959; Dettmann, 1963; Hasel de Menéndez, 1976; Archangelsky and Villar de Seoane, 1996; Archangelsky and Archangelsky, 2005). The Lycophyta are represented by *Retitriletes* sp., and *Ceratosporites* sp. (Dettmann, 1963; Srivastava, 1972; Tryon and Lugardon, 1990; Archangelsky and Villar de Seoane, 1994, 1998). The spores of Pteridophyta affinity are *Cyathidites* spp. and *Concavissimisporites* sp. (Dettmann, 1963; Fensone, 1987; Archangelsky and Villar de Seoane, 1994).
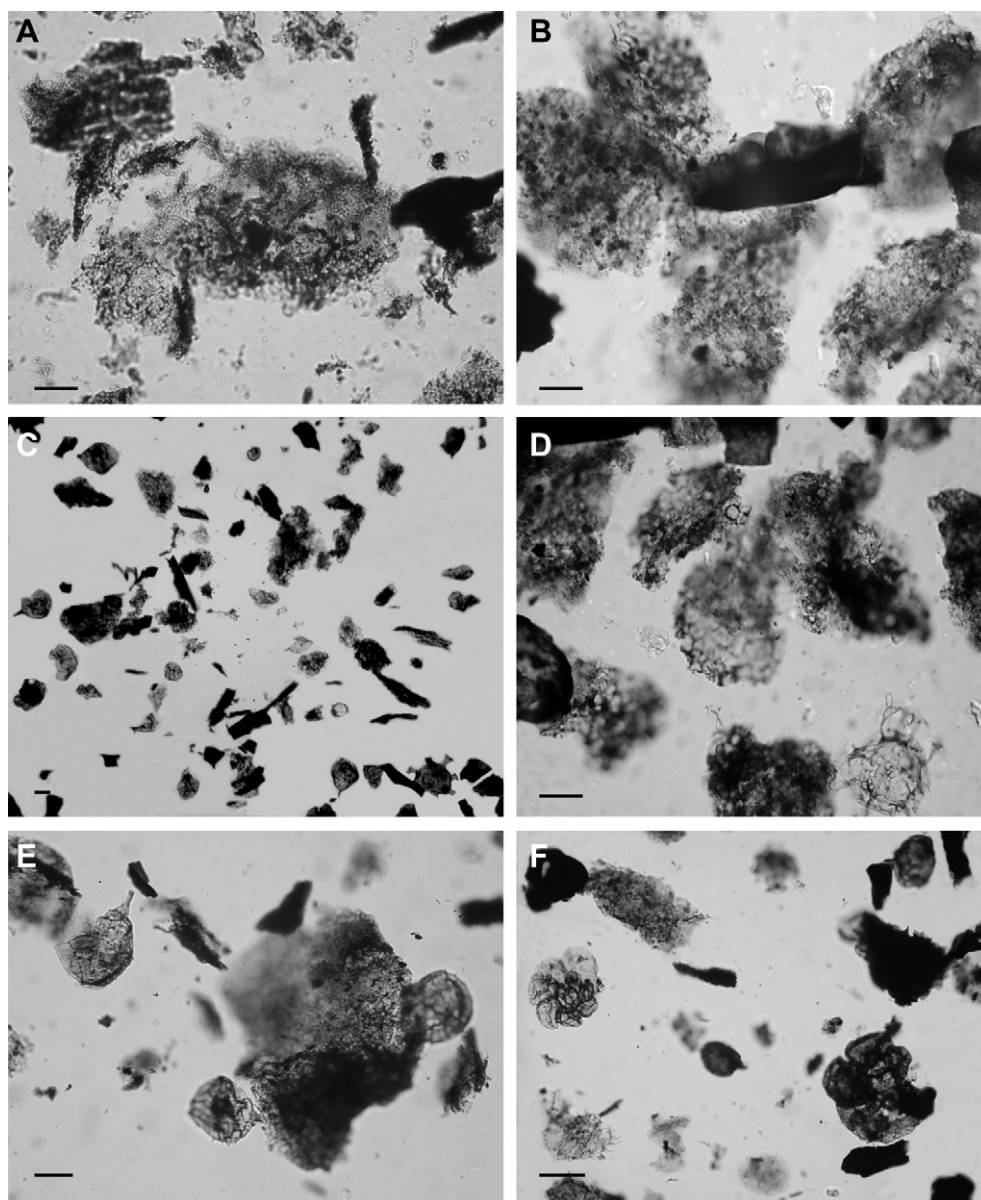
Fig. 11. Sedimentary organic matter from the Agua de la Mula Member. A, B, D, highly AOM-dominated Palynofacies 1 from levels AM3, AM4, AM2, respectively; in the basal *Spitidiscus riccardii* zone. C, E, F, AOM, *Cribroperidinium*-dominated dinoflagellate cyst assemblage, and phytoclasts characterize Palynofacies 2 at level AG3d, in the lower part of the *Crioceratites diamantensis* zone. E, AOM fragments along with specimens of *Cribroperidinium*; F, Foraminiferal linings at level AG3d. Scale bar: 50 μm

5.3. Marine palynomorphs

Organic-walled dinoflagellate cysts are the dominant marine palynomorphs. Prasinophytes and foraminiferal linings occur only in the base of the section and acritarchs remain very scarce throughout. Qualitative and quantitative analysis revealed variations in the dinoflagellate cyst assemblages, both in their relative proportions and composition. The 44 taxa identified throughout the unit are listed in Appendix B. Dinoflagellate cysts are present in most of the samples with frequencies varying between 1 and 25% of the total organic matter. They were not identified in samples AM0–4 (where assemblages are almost entirely composed by AOM) or in samples AG23a to AG26a, where dino-flagellate cysts are very rare to absent. The dinoflagellate cyst assemblages exhibit a relatively low diversity (up to 23 species in sample AG19a) and, even when dinoflagellate cysts reach the highest frequencies and outnumber miospores, the assemblages are still dominated by only a small number of taxa. Most notably, an almost monotypic assemblage of *Cribroperidinium/Apteodinium* characterizes level 12a.

The dinoflagellate cyst assemblages show a certain affinity with those from the late Hauterivian Boreal and Tethyan regions (e.g. Duxbury, 1977; Leereveld, 1997; Torricelli, 2000, 2001), but our assemblages lack any biostratigraphical markers for conclusive correlation. Nevertheless, potential local biostratigraphical signifi-cance of endemic species is observed, e.g. *Muderongia brachialis* Ottone and Pérez Loinaze, which occurs in Agua de la Mula (Ottone and Pérez Loinaze, 2002) and herein, where it is constrained to the *Spitidiscus riccardii* and lowermost *Crioceratites schlagintweiti* zones.

Palaeoenvironmental inferences based on marine paly-nomorphs were made in those intervals where dinoflagellate

Table 1
Classification and description of the sedimentary organic matter components counted in this study (*sensu* Tyson, 1995).

Categories and subcategories	Description
Phytoclasts	
Translucent	Brown, dark brown and black, equidimensional and lath-shaped translucent particles. Most of them have not internal structure and are translucent only at edges; only a few are biostructured showing tracheidal features.
Opaque	Black, equidimensional and lath-shaped particles, non-translucent up to edge. Both, translucent and opaque phytoclasts are attributed to woody debris of macrophytes.
Terrigenous palynomorphs	
Spores	Spores of pteridophytes, bryophytes and
Pollen grains	lycophytes and pollen grains of gymnosperm.
Marine palynomorphs	
Dinoflagellate cysts	Organic-walled dinoflagellate cysts (dinocysts),
Acritarchs	acritarchs and prasinophyte phycomata
Prasinophyte algae	derived from marine phytoplankton.
Foraminiferal linings	Zoomorphs, represented by dark brown inner lining of foraminifera.
Amorphous	
Amorphous Organic matter ("AOM")	Structureless granular masses, brown and orange in colour, derived from degradation of marine algae.
Gels	Structureless homogeneous particles, with rounded and sharp outlines, of terrestrial origin as the result of decomposition of land plants.

cysts, prasinophytes and/or foraminiferal linings are best represented and their frequencies mark peaks of relative abundance. Seven groups of dinoflagellate cysts were selected; six of them represent the dominant species in the different assemblages: *Oligosphaeridium* spp., *Kiokansium unituberculatum*, *Exochospharidium* spp., *Cribroperidinium/Apteodinium* spp., *Muderongia/Phoberocysta* spp. and *Circulodinium* spp. (Fig. 4). Each group includes all morphotypes related to the genus (Appendix B). A last group includes the rest of the minor taxa present in the assemblages.

In sample AM926 *Pterospermella*-type prasinophyte algae, increase their frequencies reaching up to 4% of the total organic matter, being very scarce throughout the section. Foraminiferal linings are present only in samples AM926, AG3a and AG3d associated with the presence of pyrite crystals in the AOM, phytoclasts and palynomorphs.

6. Fluorescence analysis

Using water as mounting medium, qualitative assessment of the fluorescence of the organic matter was done. In samples 3a–3d the AOM particles show moderately yellowish pale brown fluorescence and most palynomorphs show yellow bright fluorescence; the AOM is much less intensely fluorescent than palynomorphs. The interval AM0–AM4 exhibits a dominance of pale brown moderate to weakly fluorescent AOM particles and the palynomorphs are brightly fluorescent. The rest of the Agua de la Mula Member is strongly dominated by terrestrially derived-woody remains with fluorescent AOM very scarce or absent.

These AOM-rich samples from the basal *Spitidiscus riccardii* zone and the 3a–3d interval of the *Crioceratites diamantensis* zone and higher TOC values (between 1 and 3.8 wt.%) containing framboidal arrangements of pyrite were selected for auto fluorescence analysis on the whole rock. Apart from cloudy masses superimposed on the rock and fibres showing green and pale green or non-fluorescent, the AM0–AM4 samples contain droplets with yellow fluorescence

(caramel coloured in transmitted light). The 3a–3d interval exhibits green, orange and yellow fluorescence in linear arrangements.

7. Discussion

7.1. Terrestrial palynomorphs

The presence of abundant miospores in the marine Agua de la Mula Member is certainly related to the anemophyllous character of conifers that grew near the coast and produced considerable amounts of pollen grains that were supplied directly to the marine basin or via runoff. The Araucariaceae, and mainly *Araucaria*, is currently distributed irregularly through the Southern Hemisphere, living in relatively cold to temperate climates, at altitudes of 360–1200 m in the coast and Southern Andes of Chile, at altitudes of 500–1000 m in Rio Grande do Sul, Brazil, and northeast Argentina, and at 800–3300 m in Queensland, Australia, New Caledonia, and New Guinea (Florin, 1963). Extant pollen of *Araucaria* is wind-dispersed and morphologically similar to *Araucariacites australis*. Pollen grains of *Araucaria angustifolia* have been found about 25–30 km from their parental plants in the south of Brazil (Behling et al., 1997), and at only 4–5 km from their parental flora in northeast Argentina (Caccavari, 2003).

The Podocarpaceae are actually characteristic of the Southern Hemisphere but rarely share the same habitat with the Araucariaceae (Donoso, 1978; Cabrera and Willink, 1980). The podocarps produced saccate, wind-dispersed pollen grains that are in general consistently represented at long distances from their parental flora (Markgraf, 1983). The Cheirolepidiaceae is a family of plants that grew in a great variety of ecological niches (Taylor et al., 2009), but preferably occupied well-drained soils of upland slopes as well as lowlands near coastal areas associated with warm climates (Srivastava, 1976).

The preponderance and relatively good preservation of Araucaroid pollen grains throughout the section suggest an abundance of Araucariaceae near coastal areas. The high values of *Classopollis* throughout the Bajada del Agrio section also indicate that the Cheirolepidiaceae made up an important component of the local vegetation. The relatively low values of pollen of Podocarpaceae may imply that the group grew in a place relatively distant from the coast or elsewhere. The coeval presence of a rich coniferous-dominated flora and bioherms (Lazo et al., 2005) in the Agua de la Mula Member suggests a warm climate.

7.2. Marine-derived components, T/M ratio and paleoenvironment

The highly AOM-dominated palynofacies associated with the highest TOC values (Fig. 4) and moderately preserved AOM particles imply low oxygenated, dysoxic basinal marine environments for the basal thin laminated black shales of the *Spitidiscus riccardii* zone. As noted by Tyson et al. (2005), the presence of gastropod-bearing layers (*Protohemichenopus neuquensis*) at Pichi Mula, confirms dysoxia, rather than anoxia. In both modern and ancient sediments AOM percentages are typically lower in shallow inner shelf facies and tend to increase in darker and more organic-rich offshore sediments, associated with lower energy and lower oxygenation (Tyson, 1995; Batten, 1996). Organic-rich thin laminated black shales point out to a very quiet environment, developed below the storm wave base in a basinal to outer shelf setting. Well-preserved fossils and the presence of a low-diverse benthic association of small-sized shells support low energy and oxygen-controlled substrate for the *Spitidiscus* shales.

The Cretaceous anoxic events recorded in southern South America do not coincide with the global anoxic events for this period (Aguirre-Urreta et al., 2008). Moreover, Valanginian–Hauterivian black shales facies are rare worldwide (Tyson et al., 2005). Nevertheless, the

enclosed configuration of the Neuquén Basin and the presence of a volcanic arc on its western margin would have generated (at least temporarily) the isolation of the basin from the Pacific Ocean (e.g. Veiga et al. 2005). This fact along with the consequent reduced circulation would have favoured the development of stratified water-masses and dysoxia–anoxia during the two most important transgressive episodes in the Agrio Formation. The first one produced the late Valanginian black shales of the Pilmatué Member and the second one the late Hauterivian *Spitidiscus* shales of the Agua de la Mula Member. A widespread phenomenon equivalent of the late Hauterivian Faraoni event has been proposed by Archuby et al. (2011) for a thin package of dark grey and black mudrocks in the *Crioceratites diamantensis* zone of the Agua de la Mula Member. However, as this was identified in only two localities within the basin, a correlation with the Faraoni event remains speculative and requires confirmation.

The dark grey shales of the AG3a–3d interval from the lower part of the *Crioceratites diamantensis* zone are characterized by marine-derived AOM-rich palynofacies. However, they clearly differ from the *Spitidiscus* shales because of the relative increase in phytoclast and dinoflagellate cysts, less preservation of the AOM particles (weak to non-fluorescent) and the presence of pavements of large oysters and inoceramid bivalves, suggesting more dysoxic to oxic seafloors in an outer shelf setting.

For the rest of the Agua de la Mula Member the sedimentary organic matter is strongly dominated by phytoclasts, reflecting proximity to the source of terrestrial organic matter and/or, oxidizing environments with the selective destruction of other components (Tyson, 1995). The T/M ratio shows a highly fluctuating marine and terrestrial influence through most of the *Crioceratites schlagintweiti* and *C. diamantensis* zones (Fig. 5). The relative abundance of terrestrial and marine palynomorphs have been widely used to indicate transgressive–regressive trends and distances from the coastline (e.g. Lister and Batten, 1988; Stover et al., 1996; Harker et al., 1990; Prauss, 2001; Götz et al., 2008). However, there is not a clear trend, as the T/M parameter presents a rather noisy signal, except at the top of the section where several parameters show a consistent proximal trend and the increase in the proportion of terrestrial palynomorphs (highest T/M) correlates with highest proportions of tetrads of Cheirolepidiaceae and spores (highest spore/bisaccate ratio) (Palynofacies 1). These trends suggest the most basinward position of the coastline and besides, higher representation of pollen aggregates due to a short and relatively low energy transport from the terrestrial source area (Tyson, 1995 and references therein).

The phytoclast-dominated Palynofacies 2, 3 and 4 that characterize the middle part of the section (approximately between 150 and 400 m), particularly those with lower T/M ratio, suggest well oxygenated inner shelf environments. The presence of highly diverse macrobenthos and high bioturbation in these intervals denote oxygenated seafloor conditions. Dinoflagellate cyst assemblages are of moderate to low diversity, with high dominance in most of the cases. Modern patterns of dinoflagellate cyst distribution have demonstrated that besides the nutrient availability, the diversity is highly controlled by the stress of the ecosystems, decreasing from neritic/oceanic to coastal environments (e.g. Wall et al., 1977; Pross and Brinkhuis, 2005). Thus, dinoflagellate cyst assemblages suggest an overall shallow water, inner shelf environment, with a probable stressed photic zone in some cases (e.g. *Cribroperidinium*-dominated level 12a), typical of unstable coastal and marginal settings (Pross and Brinkhuis, 2005).

7.1. Maturity, preservation and hydrocarbon potential

Amorphous organic matter is the most important and abundant oil-prone constituent in the majority of the petroleum source rocks, especially in distal marine or lacustrine facies (Tyson, 1995). The preservation state of the AOM, reflected by its degree of fluorescence, is critical for evaluating the hydrocarbon generating potential (Tyson, 1995; 2006). For thermally immature to early mature rocks, there is typically a positive correlation between percentages of AOM, fluorescence intensity and hydrogen index – the pyrolytic yield of hydrocarbons normalized to the sample TOC, mgHC/gTOC (Tyson, 2006). In this study, the degree of fluorescence of the organic matter was analysed in the two organic-rich intervals AM0–AM4 (*S. riccardii* zone) and AG3a–d (lower third the *C. diamantensis* Zone), where AOM content is higher than 65% and the TOC values around 1 wt.% or higher. The rest of the Agua de la Mula Member is mostly composed by non-fluorescent phytoclasts and palynomorphs, indicating poor preservation related to the oxic proximal marine facies (see 7.2). The basal AM0–AM4 interval shows AOM with a dominance of a relatively moderate fluorescence of yellowish pale brown colour, whereas the palynomorphs are bright fluorescent. According to the six-point qualitative preservation scale of Tyson (1995) samples of the AM0–AM4 interval would have a fluorescence scale value 4, typically associated with Type II kerogen. Based on their organic facies analysis, Tyson et al. (2005) suggested a Type II/III kerogen and an early mature character for the *Spitidiscus riccardii* shales in the Chos Malal area. In the 3a–3d interval, AOM particles are predominantly moderate to weak and non-fluorescent whereas the palynomorphs show a yellow bright fluorescence. These samples might have fluorescence scale value 2b or 3, associated with Type IV/III or Type III/II kerogen (Tyson, 1995). The fact that the AOM particles are much less intensely fluorescent than the palynomorphs indicates a partially degraded AOM, in agreement with the dysoxic to oxic conditions indicated for this interval (See 7.2). The predominance of yellow and green fluorescence colours suggests the rocks are no more than early mature. Maturation results in a progressive change in visual fluorescence colour from green or yellow to orange or brown, accompanied by an overall decrease in fluorescence intensity (van Gijzel, 1979; Robert, 1988) until sporomorph and AOM visual fluorescence is lost at a maturity of around 0.8–1.0% vitrinite reflectance in the late oil window (Collins, 1990), although that of telalginitic algae such as *Botryococcus* and prasinophytes may persist a little beyond this. Fluorescence observations also provide information about maturity of the generated products, when the whole rock is observed (Riecker, 1962). In sample AG3d, gold yellow fluorescence occurs in arcuate linear features suggesting migrant oil microfractures. Likewise, weak golden yellow fluorescent spherical-shaped bodies were observed in the basal samples AM0–4. These hydrocarbons are either very early generated *in situ* product associated with the expulsion time or allochthonous and derived from a deeper source rock, although if the latter it is difficult to envisage how migration could have occurred through the underlying shale-dominated succession.

7.4. Palynofacies and sequence stratigraphy

In the studied section four depositional sequences (SQ1–SQ4) were documented (Fig. 2) as part of a lower frequency mesosequence. The TST1 of the first depositional sequence (SQ1) coincides entirely with the TST of the mesosequence. It is characterized by the dark organic-rich shales of the *Spitidiscus riccardii* zone (late Hauterivian) containing the AOM-dominated Palynofacies 6, which undoubtedly marks the most significant flooding episode during deposition of the Agua de la Mula Member; as basal offshore marine deposits lie directly upon the fluvial and aeolian sandstones of the Avilé Member, previously deposited during a forced

regression (Veiga et al., 2002). TST1 represents a widespread regional marine transgression in the basin, linked to a rapid inundation due to a sea level rise.

TST2 of the second depositional sequence (SQ2) is interpreted in the AG3a–6a interval from the basal part of the *Crioceratites diamantensis* zone (Fig. 2). The AOM and dinoflagellate cyst-dominated assemblages (Palynofacies 5) in the lower part of the TST2 and the increased dinoflagellate cyst proportions in samples AG5a and AG5b samples in phytoclast-dominated assemblages (Palynofacies 1B), along with pavements of inoceramids and oysters, might be indicative of several stacked transgressive surfaces, linked to pauses in the sedimentation or minor punctuated floodings with sediment starvation in the outer ramp. A regressive interval with abrupt reduction in the marine components would separate these two transgressive pulses. Inoceramid bivalves are commonly related to dysoxic to suboxic (exaerobic) seafloors but in this case they alternate with oxic substrates colonized by large oysters. The base of TST2 coincides with the replacement of the *Crioceratites schlagintweiti* zone ammonoids by the *C. diamantensis* zone ones.

The third and fourth TSTs (TST3 and TST4) recognized in the middle and upper part of the *C. diamantensis* zone, are represented in the AG12a–14b and AG17a–19a intervals, respectively (Fig. 2). Palynologically, TST3 and TST4 do not show a significantly different signal, just the higher phy/spm ratios that characterize Palynofacies 2. However, in TST4, Palynofacies 2 shows the lowest T/M ratio, with higher dinoflagellate cyst percentages and diversity and the highest proportion of bisaccates is observed (lowest spore/bisaccate ratio). The last major flooding event during deposition of the Agua de la Mula Member seems to occur in TST4 and is followed by a strongly continental-influenced interval. Changes in the organic matter composition (mainly a decrease in marine-derived AOM) imply a change in the depositional conditions from offshore anoxic conditions in TST1 to more oxygenated, presumably shallower proximal settings in TST4. Similarly, the unusual depauperate small-sized benthic fauna suggests an oxygen-controlled distal setting in TST1, while the subsequent larger and more diverse benthic shell bed macrofauna indicate progressively more oxygenated conditions in TST2, TST3 and TST4. In the same way, the stratigraphical distribution of the palynofacies suggests an overall distal to proximal, upward regressive trend that might be associated with a reduction of the accommodation space. The oxygen-controlled settings linked to the basinal or distal portion of an overall shallow marine ramp, would probably have been deposited in depths less than 100 m. TST1 is the fourth-order transgressive system tract (SQ1), but also is coincident with the TST of the third order sequence or "Upper Mendoza Mesosequence" after the sea level fall recorded in the Avilé Member (LST). The thick phytoclast-dominated overlying succession represents the highstand of this third order sequence. Therefore, superimposed on this third order highstand, the other four depositional sequences, SQ1, SQ2, SQ3 and SQ4, represent high frequency fluctuations in the sea level, and probably of fourth-order hierarchy.

8. Conclusions

Variations in the content and composition of the sedimentary organic matter combined with macrofaunal analysis permit an interpretation of the environmental conditions during deposition of the Agua de la Mula Member of the Agrio Formation. Organic-rich AOM-dominated palynofacies are restricted to the *Spitidiscus riccardii* zone and the lowermost part of the *Crioceratites diamantensis* zone and correlate with the highest TOC values. Terrestrially-derived-dominated palynofacies characterize the rest

of the Agua de la Mula Member and coincide with the lowest TOC values (less than 1 wt.%).

The organic-rich thin laminated black shales of the *Spitidiscus riccardii* zone constitute a major transgressive systems tract (TST) related to a third order sequence but also coincident with the TST1 of the lower order sequence (SQ1). The HST1 of the first sequence (SQ1) and another three depositional sequences (SQ2–SQ4) all of them of higher order and frequency (probably fourth order), are included in the overlying thick third order highstand systems tract (HST).

Each described sequence is composed of a transgressive systems tract (TST1–TST4) and a highstand systems tract (HST1–HST4); noticeably, only a one-lowstand system tract was recognized. However it is related to the third order sequence also known as " Upper Mendoza Mesosequence". The TST2 is characterized by increased marine-derived AOM and dinoflagellate cysts, whereas TST3 and TST4 as well the HSTs are dominated by terrestrially-derived components, mostly phytoclasts. Particularly, TST3 and TST4 do not show other distinctive palynological signal than the lowest T/M and spore/bisaccate ratios. Oxygen-controlled, basinal and outer ramp settings were indicated for the TST1 and the lower TST2, respectively. The rest of the sedimentary succession, suggests the prevalence of well oxygenated, middle to inner ramp depositional environments, with an overall high terrestrial input from the adjacent land areas. This scenario agrees with a low gradient ramp setting and the proximal location of the study section, close to the southern boundary of the basin.

Decreasing TOC, AOM content and preservation state of the organic matter is associated with improved oxygenation, due to a distal to proximal, shallowing-upward trend recorded through the section.

The evidence of hydrocarbon droplets and hydrocarbon stained fractures in the predominantly immature Agua de la Mula Member, suggest early generation of liquid hydrocarbon products reaching the expulsion time.

References

Aguirre-Urreta, M.B., Rawson, P.F., Concheyro, G.A., Bown, P.R., Ottone, E.G., 2005. Lower Cretaceous (Berriasian − Aptian) biostratigraphy of the Neuquén Basin. In: Veiga, G.D., Spalletti, L.A., Howell, J.A., Schwarz, E. (Eds.), The Neuquén Basin, Argentina: A case study in sequence stratigraphy and basin dynamics. Geological Society of London, Special Publications 252, pp. 57–81.

Aguirre-Urreta, M.B., Amaro Mourgues, F., Rawson, P.F., Bulot, L.G., Jaillard, E., 2007. The Lower Cretaceous Chañarcillo and Neuquén Andean Basins: ammonoid biostratigraphy and correlations. Geological Journal 42, 143–173.

Aguirre-Urreta, M.B., Price, G.D., Ruffell, A.H., Lazo, D.G., Kalin, R.M., Ogle, N., Rawson, P.F., 2008. Southern Hemisphere Early Cretaceous (Valanginian-Early Barremian) carbon and oxygen isotope curves from the Neuquén Basin, Argentina. Cretaceous Research 29, 87–99.

Archangelsky, S., 1966. New gymnosperms from the Tico Flora, Santa Cruz province, Argentina. Bulletin of the British Museum (Natural History) Geology 13, 259–295.

Archangelsky, S., 1977. *Balmeiopsis*, nuevo nombre para el palinomorfo *Inaperturopollenites limbatus* Balme, 1957. Ameghiniana 14, 122–126.

Archangelsky, S., 1994. Comparative ultrastructure of three Early Cretaceous gymnosperm pollen grains: *Araucariacites, Balmeiopsis* and *Callialasporites*. Review of Palaeobotany and Palynology 83, 185–198.

Archangelsky, S., Archangelsky, A., 2005. *Aequitriradites* Delcourt & Sprumont y *Couperisporites* Pocock, esporas de hepáticas, en el Cretácico Temprano de Patagonia, Argentina. Revista del Museo Argentino de Ciencias Naturales, nueva serie 7, 119–138.

Archangelsky, S., Villar de Seoane, L., 1994. Estudios palinológicos de la Formación Baqueró (Cretácico), provincia de Santa Cruz, Argentina. VI. Ameghiniana 31, 41–53.

Archangelsky, S., Villar de Seoane, L., 1996. Estudios palinológicos de la Formación Baqueró (Cretácico), provincia de Santa Cruz, Argentina. VII. Ameghiniana 33, 307–313.

Archangelsky, S., Villar de Seoane, L., 1998. Estudios palinológicos de la Formación Baqueró (Cretácico), provincia de Santa Cruz, Argentina. VIII. Ameghiniana 35, 7–19.

Archangelsky, S., Villar de Seoane, L., 2005. Estudios palinológicos del Grupo Baqueró (Cretácico Inferior), provincia de Santa Cruz, Argentina. IX polen bisacado de Podocarpaceae. Revista Española de Paleontología 20, 37–56.

Archuby, F.M., Wilmsen, M., Leanza, H.A., 2011. Integrated stratigraphy of the Upper Hauterivian to Lower Barremian Agua de la Mula Member of the Agrio Formation, Neuquen Basin, Argentina. Acta Geologica Polonica 61, 1–26.

Baldoni, A.M., 1979. Nuevos elementos paleoflorísticos de la tafoflora de la Formación Springhill, límite Jurásico-Cretácico, subsuelo de Argentina y Chile austral. Ameghiniana 16, 103–119.

Balme, B.E., 1957. Spores and pollen grains from the Mesozoic of Western Australia. Commonwealth Scientific and Industrial Research Organization of Australia (CSIRO). Coal Research Section 25, 1–48.

Balme, B.E., 1995. Fossil in situ spores and pollen grains: an annotated catalogue. Review of Palaeobotany and Palynology 87, 81–323.

Banerjee, I., Kidwell, S.M., 1991. Significance of molluscan shell beds in sequence Stratigraphy: an example from the Lower Cretaceous Manville Group of Canada. Sedimentology 38, 913–934.

Batten, D.J., 1996. Palynofacies and palaeoenvironmental interpretation. In: Jansonius, J., McGregor, D.C. (Eds.), Palynology: principles and applications. American Association of Stratigraphic Palynologists Foundation 3, pp. 1011–1064.

Batten, D.J., Dutta, R.J., 1997. Ultrastructure of exine of gymnospermous pollen grains from Jurassic and basal Cretaceous deposits in Northwest Europe and implications for botanical relationships. Review of Palaeobotany and Palynology 99, 25–54.

Behling, H., Negrelle, R.R.B., Colinvaux, P.A., 1997. Modern pollen rain data from the tropical Atlantic rain forest, Reserva Volta Velha, South Brazil. Review of Palaeobotany and Palynology 97, 287–299.

Cabrera, A.L., Willink, A., 1980. Biogeografía de América Latina. In: Biología, Serie, Segunda (Eds.). Secretaría General de la Organización de los Estados Americanos, Washington.

Caccavari, M.A., 2003. Dispersión del polen de Araucaria angustifolia (Bert.) O. Ktze. 12 Simposio Argentino de Paleobotánica y Palinología, (Buenos Aires), Resúmenes, 10.

Collins, A., 1990. The 1–10 spore colour index (SCI) scale: a universally applicable colour maturation scale, based on graded, picked palynomorphs. In: Fermont, W.J.J., Weegink, J.W. (Eds.), Proceedings of the International Symposium on Organic Petrology, Zeist, The Netherlands. Mededelingen Rijks Geologische Dienst 45, pp. 39–47.

Cruz, C.E., Villar, H.J., Muñoz, G.N., 1996. Los sistemas petroleros del Grupo Mendoza en la fosa de Chos Malal. Cuenca Neuquina, Argentina. In: XIII Congreso Geológico Argentino y III Congreso de Exploración de Hidrocarburos, Actas, pp. 45–60.

Cruz, C.E., Kozlowski, E., Villar, H.J., 1998. Agrio (Neocomian) petroleum systems: main target in the Neuquén Basin thrust belt. American Association of Petroleum Geologists International Conference & Exhibition Extended Abstracts, 670–671.

Del Fueyo, G., 1991. Una nueva Araucariaceae cretácica de Patagonia, Argentina. Ameghiniana 28, 149–161.

Del Fueyo, G., Archangelsky, S., 2005. A new araucarian pollen cone with in situ *Cyclusphaera* Elsik from the Aptian of Patagonia, Argentina. Cretaceous Research 26, 757–768.

Dettmann, M.E., 1963. Upper Mesozoic microfloras from South-Eastern Australia. Proceedings of the Royal Society of Victoria 77, 1–148.

Dettmann, M.E., Jarzen, D.M., 2000. Pollen of extant *Wollemia* (wollemi pine) and comparisons with pollen of other extant and fossil Araucariaceae. In: Harley, M.M., Morton, C.M., Blackmore, S. (Eds.), Pollen and spores: morphology and biology. The Royal Botanic Gardens, Kew, pp. 187–203.

Donoso, C., 1978. Dendrología, árboles y arbustos chilenos. Universidad de Chile, Facultad de Ciencias Forestales, Manual 2, 43 p.

Duxbury, S., 1977. A palynostratigraphy of the Berriasian to Barremian of the Speeton Clay of Speeton, England. Palaeontographica B 160, 17–67.

Fensone, R.A., 1987. Taxonomy and biostratigraphy of schizaealean spores from the Jurassic-Cretaceous boundary beds of the Aklavik Range, District of Mackenzie. Palaeontographica Canadiana 4, 1–50.

Fensome, R.A., Williams, G.L., 2004. The Lentin and Williams index of fossil dinoflagellates. American Association of Stratigraphic Palynologists Foundation, Contribution Series 42, p. 909.

Florin, R., 1963. The distribution of conifer and taxa genera in time and space. Acta Horti Bergiani 20, 121–136.

Gamerro, J.C., 1965. Morfología del polen de *Apterocladus lanceolatus* Archang. (Coniferae) de la Formación Baqueró, provincia de Santa Cruz. Ameghiniana 4, 133–138.

Götz, A.E., Feist-Burkhardt, S., Ruckwied, K., 2008. Palynofacies and sea-level changes in the Upper Cretaceous of the Vocontian Basin, Southeast France. Cretaceous Research 29, 1047–1057.

Grimm, E., 1991–93. Tilia Software. Illinois State Museum. Research and Collection Center, Springfield, Illinois.

Harker, S.D., Sarjeant, W.A.S., Caldwell, W.G.E., 1990. Late Cretaceous (Campanian) organic-walled microplankton from the interior plains of Canada, Wyoming and Texas: biostratigraphy, palaeontology and palaeoenvironmental interpretation. Palaeontographica, Abteilung B 219, 243.

Hasel de Menéndez, G.G., 1976. Taxonomic problems and progress in the study of the Hepaticae. The Journal of the Hattori Botanical Laboratory 41, 19–36.

Helland-Hansen, W., Martinsen, O.J., 1996. Shoreline trajectories and sequences: description of variable depositional-dip scenarios. Journal of Sedimentary Research 66, 670–688.

Howell, J.A., Schwarz, E., Spalletti, L.A., Veiga, G.D., 2005. The Neuquén Basin: an overview. In: Veiga, G.D., Spalletti, L.A., Howell, J.A., Schwarz, E. (Eds.), The Neuquén Basin, Argentina: A case study in sequence stratigraphy and basin dynamics. Geological Society of London, Special Publications 252, pp. 1–14.

Krutzsch, W., 1959. Mikropaläontologische (sporenpaläontologische) Untersuchungen in der Braunkohle des Geiseltales. I. Die Sporen und die sporenartigen sowie ehemals im Geiseltal zu Sporites gestellen Formeinheiten der Sporae dispersae der mitteleozänen Braunkohle des mittleren Geiseltales (Tagebau Neumark-West i. w. S), unter Berücksichtigung und Revision weiterer Sporenformen aus der bisherigen Literatur. Geologie 21–22, 1–425.

Lazo, D.G., 2006. Análisis tafonómico e inferencia del grado de mezcla temporal y espacial de la macrofauna del Miembro Pilmatué de la Formación Agrio, Cretácico Inferior de cuenca Neuquina, Argentina. Ameghiniana 43, 311–326.

Lazo, D.G., 2007. Análisis de biofacies y cambios relativos del nivel del mar en el Miembro Pilmatué de la Formación Agrio, Cretácico Inferior de cuenca Neuquina, Argentina. Ameghiniana 44, 73–89.

Lazo, D.G., Cichowolski, M., Rodríguez, D.L., Aguirre-Urreta, M.B., 2005. Lithofacies, palaeoecology and plaeoenvironments of the Agrio Formation, Lower Cretaceous of the Neuquén Basin, Argentina. In: Veiga, G.D., Spalletti, L.A., Howell, J.A., Schwarz, E. (Eds.), The Neuquén Basin, Argentina: a case study in sequence stratigraphy and basin dynamics. Geological Society, London, Special Publications 252, pp. 295–315.

Leanza, H.A., Hugo, C.A., 2001. Cretaceous red beds from southern Neuquén Basin (Argentina): age, distribution and stratigraphic discontinuities. In: 7° International Symposium on Mesozoic Terrestrial Ecosystems. Asociación Paleontológica Argentina, Publicación Especial 7, pp. 117–122.

Legarreta, L., Gulisano, C.A., 1989. Análisis estratigráfico secuencial de la Cuenca Neuquina (Triásico Superior–Terciario Inferior, Argentina). In: Chebli, G.A., Spalletti, L.A. (Eds.), Cuencas Sedimentarias Argentinas, Simposio de Cuencas Sedimentarias Argentinas, X Congreso Geológico Argentino, Tucumán, pp. 221–243.

Legarreta, L., Uliana, M.A., 1991. Jurassic-Cretaceous marine oscillations and geometry of a back-arc basin fill, central Argentine Andes. In: MacDonald, D.I.M. (Ed.), Sedimentation, Tectonics and Eustacy. Sea Level Changes at Active Margins. International Association of Sedimentologists, Special Publication 12, pp. 429–450.

Leereveld, H., 1997. Hauterivian–Barremian (Lower Cretaceous) dinoflagellate cyst stratigraphy of the western Mediterranean. Cretaceous Research 18, 421–456.

Lister, J.K., Batten, D.J., 1988. Stratigraphical and palaeoenvironmental distribution of Early Cretaceous dinoflagellate cysts in the Hurlands Farm Borehole, West Sussex, England. Palaeontographica 210 B, 9–89.

Markgraf, V., 1983. Late and postglacial vegetational and paleoclimatic changes in subantarctic, temperate, and arid environments in Argentina. Palynology 7, 43–70.

Ottone, E.G., Pérez Loinaze, V.S., 2002. A new dinoflagellate from the Lower Cretaceous of Argentina. Ameghiniana 39, 117–120.

Pazos, P.J., Lazo, D.G., Tunik, M.A., Marsicano, C.A., Fernandez, D.E., Aguirre-Urreta, M.B., 2012. Paleoenvironmetal framework of dinosaur tracksites and other ichnofossils in Early Cretaceous mixed siliciclastic-carbonate deposits in the Neuquen Basin, northern Patagonia (Argentina). Gondwana Research 22, 1125–1140.

Prauss, M.L., 2001. Sea-level changes and organic walled phytoplankton response in a late Albian epicontinental setting, Lower Saxony Basin, NW Germany. Palaeogeography, Palaeoclimatology, Palaeoecology 174, 221–249.

Pross, J., Brinkhuis, H., 2005. Organic-walled dinoflagellate cysts as paleoenvironmental indicators in the Paleogene; a synopsis of concepts. Paläontologische Zeitschrift 79, 53–59.

Ramos, E.G., Folguera, A., 2005. Tectonic evolution of the Andes of Neuquén: Constraints derived from the magmatic arc and foreland deformation. In: Veiga, G.D., Spalletti, L.A., Howell, J.A., Schwarz, E. (Eds.), The Neuquén Basin, Argentina: A case study in sequence stratigraphy and basin dynamics. Geological Society of London, Special Publications 252, pp. 15–35.

Riecker, R.E., 1962. Hydrocarbon fluorescence and migration of petroleum. American Association of Petroleum Geologists, Bulletin 46, 60–75.

Robert, P., 1988. Organic metamorphism and geothermal history: microscopic study of organic matter and thermal evolution of sedimentary basins. Reidel Publishing, Dordrecht, Netherlands.

Spalletti, L.A., Poiré, D.G., Schwarz, E., Veiga, G.D., 2001. Sedimentologic and sequence stratigraphic model of a Neocomian marine carbonate–siliciclastic ramp: Neuquén Basin, Argentina. Journal of South American Earth Sciences 14, 609–624.

Srivastava, S.K., 1972. Systematic description of some spores from the Edmonton Formation (Maestrichtian), Alberta, Canada. Palaeontographica 139 B, 1–46.

Srivastava, S.K., 1976. The fossil pollen genus *Classopollis*. Lethaia 9, 437–457.

Stover, L.E., Brinkhuis, H., Damassa, S.P., de Verteuil, R.J., Helby, R.J., Monteil, E., Partridge, A.D., Powell, A.J., Riding, J.B., Smelror, M., Williams, G.L., 1996. Mesozoic-Tertiary dinoflagellates, acritarchs and prasinophytes. In: Jansonius, J., McGregor, D.C. (Eds.), Palynology: principles and applications. American Association of Stratigraphic Palynologists Foundation 2, pp. 641–750.

Taylor, T.N., Taylor, E.L., Krings, M., 2009. Paleobotany. The biology and evolution of fossil plants, second ed. Academic Press, Burlington.

Torricelli, S., 2000. Lower Cretaceous dinoflagellate cyst and acritarch stratigraphy of the Cismon APTICORE (Southern Alps, Italy). Review of Palaeobotany and Palynology 108, 213–266.

Torricelli, S., 2001. Dinoflagellate cyst stratigraphy of the Lower Cretaceous Monto Soro Flysch in Sicily (Italy). Rivista Italiana di Paleontologia e Stratigrafia 107, 79–105.

Townrow, J.A., 1967. On a conifer from the Jurassic of East Antarctica. Papers and Proceedings of the Royal Society of Tasmania 101, 137–148.

Tryon, A.F., Lugardon, B., 1990. Spores of the Pteridophyta. Surface, wall structure, and diversity based on electron microscopic studies. Springer-Verlag.

Tyson, R.V., 1995. Sedimentary organic matter. Organic facies and palynofacies. Chapman and Hall, London.

Tyson, R.V., 2006. Calibration of hydrogen indices with microscopy: a review, reanalysis and new results using fluorescence scale. Organic Geochemistry 37, 45–63.

Tyson, R.V., Esherwood, P., Pattison, K.A., 2005. Organic facies variations in the Valanginian-mid-Hauterivian interval of the Agrio Formation (Chos Malal area, Neuquén, Argentina): local significance and global context. In: Veiga, G.D., Spalletti, L.A., Howell, J.A., Schwarz, E. (Eds.), The Neuquén Basin, Argentina: A case study in sequence stratigraphy and basin dynamics. Geological Society of London, Special Publications 252, pp. 251–266.

Uliana, M.A., Legarreta, L., 1993. Hydrocarbon habitat in a Triassic-to-Cretaceous sub-Andean setting: Neuquén Basin, Argentina. Journal of Petroleum Geology 16, 397–420.

Uliana, M.A., Legarreta, L., Laffitte, G.A., Villar, H., 1999. Estratigrafía y geoquímica de las facies generadoras de hidrocarburos en las cuencas petrolíferas de Argentina. In: 4° Congreso de Exploración y Desarrollo de Hidrocarburos, Actas, 1-61, Buenos Aires.

van Gijzel, P., October 1979. Manual of the techniques and some geological applications of fluorescence microscopy. Workshop. American Association of Stratigraphic Palynologists Foundation, Dallas.

van Konijnenburg-van Cittert, J.H.A., 1971. In situ gymnosperm pollen from the Middle Jurassic of Yorkshire. Acta Botanica Neerlandica 20, 1–96.

Veiga, G.D., Spalletti, L.A., Flint, S., 2002. Aeolian/fluvial interactions and high-resolution sequence stratigraphy of a non-marine lowstand wedge: the Avilé Member of the Agrio Formation (Lower Cretaceous), central Neuquén Basin, Argentina. Sedimentology 49, 1001–1019.

Veiga, G.D., Howell, J.A., Strömbäck, A., 2005. Anatomy of a mixed marine-non marine lowstand wedge in a ramp setting. The record of a Barremian-Aptian complex relatively sea-level fall in the central Neuquen Basin, Argentina. In: Veiga, G.D., Spalletti, L.A., Howell, J.A., Schwarz, E. (Eds.), The Neuquén Basin, Argentina: a case study in sequence stratigraphy and basin dynamics. Geological Society, London, Special Publications 252, pp. 139–162.

Wall, D., Dale, B., Lohmann, G.P., Smith, W.K., 1977. The environmental and climatic distribution of dinoflagellate cysts in modern marine sediments from regions in North and South Atlantic Oceans and adjacent areas. Marine Micropaleontology 2, 121–200.

Weaver, C.E., 1931. Paleontology of the Jurassic and Cretaceous of West Central Argentina. In: Memoir of the University of Washington 1, 1–469.

Appendix A

List of pollen and spores taxa recognized in the Agua de la Mula Member of the Agrio Formation.

DIVISION BRYOPHYTA
Aequitriradites sp.
Foraminisporis sp.
Foraminisporis sp. cf. *F. wonthaggiensis* (Cookson and Dettmann) Dettmann 1963
Nevesisporites radiatus (Chlonova) Srivastava 1972r Fig. 6A,E
DIVISION BRYOPHYTA?
Interulobites intraverrucatus Phillips in Phillips and Felix 1971 Fig.6F
DIVISION LYCOPHYTA
FAMILY LYCOPODIACEAE
Retitriletes sp. Fig. 6G

FAMILY SELLAGINELACEAE
Ceratosporites sp. Fig. 6D
DIVISION PTERIDOPHYTA
Familia Cyatheaceae-Dicksoniaceae
Cyathidites australis Couper 1953
Cyathidites sp.
FAMILY SCHIZACEAE
Concavissimisporites spp. Fig. 6C
DIVISION CONIFEROPHYTA
FAMILY ARAUCARIACEAE
Araucariacites australis Cookson 1947 Fig. 6L.P
Balmeiopsis limbatus (Balme) Archangelsky 1977 Fig. 6K
Callialasporites dampieri (Balme) Dev 1961
Callialasporites trilobatus (Balme) Dev 1961 Fig.6I
Callialasporites turbatus (Balme) Schulz 1967 Fig. 6J
Cyclusphaera psilata Volkheimer and Sepúlveda 1976 Fig. 6N
Cyclusphaera radiata Archangelsky in Archangelsky et al. 1984 Fig. 6M,O
FAMILY PODOCARPACEAE
Podocarpidites sp.
FAMILY CHEIROLEPIDIACEAE
Classopollis sp. Fig. 6H

Appendix B

List of the dinoflagellate cysts taxa recognized in the Agua de la Mula Member of the Agrio Formation. References correspond to Fensome and Williams (2004).

ORDER GONYAULACALES
FAMILY GANYAULACACEAE
Apteodinium granulatum Eisenack 1958a Jan du Chêne et al. 1986b
Apteodinium sp.
Callaiosphaeridium cf. *asymmetricum* (Deflandre and Courteville 1939) Davey and Williams 1966b emend Clarke and Verdier 1967
Cribroperidinium edwarsii Cookson and Eisenack 1958) Davey 1969a
Cribroperidinium orthoceras (Eisenack 1958) Davey 1969 Fig. 7H
Cribroperidinium spp.
Dingodinium cerviculum Cookson and Eisenack 1958 *emend.* Khowaja-Ateequezzaman et al. 1990 Fig. 7G
Exochosphaeridium bifidum (Clarke and Verdier 1967) Clark et al. 1968 *emend* Davey 1969b
Exochosphaeridium phragmites Davey et al. 1966
Exochosphaeridium sp.
Florentinia mantellii (Davey and Williams 1966) Davey and Verdier 1973
Florentinia sp.
Gonyaulacysta spp.
Hystrichodinium pulchrum Deflandre 1935
Hystrichosphaerina schindewolfii Alberti 1961
Kallosphaeridium sp. Fig. 7D
Kiokansium unituberculatum (Tasch in Tasch et al. 1964) Stover and Evitt 1978
Lithodinia sp.
Mendicodinium sp. Fig. 7C
Occisucysta tentoria Duxbury 1977 *emend.* Jan du Chêne et al. 1986b Fig. 7F
Oligosphaeridium complex (White 1842) Davey and Williams 1966 Fig. 7A
Oligosphaeridium poculum Jain 1977b
Oligosphaeridium pulcherrimun (Deflandre and Cookson 1955) Davey and Williams 1966b
Oligosphaeridium cf. *dividuum* Williams 1978
Rhynchodiniopsis sp.
Scrinodinium sp.
Spiniferites spp.
Systematophora sp.
Tanyosphaeridium magneticum Davies 1983 *emend.* Torricelli 2000 Fig. 7I
Tanyosphaeridium salpinx Norvick 1976
Tanyosphaeridium cf. *isocalamum* (Deflandre and Cookson 1955) Davey and Williams 1969
Tehamadinium cf. *sousensis* (Below 1981) Jan du Chêne et al. 1986b
Tehamadinium sp.
FAMILY AREOLIGERACEAE
Canningia cf. *pistica* Helby 1987
Cerbia tabulata Davey and Verdier 1974) Below 1981a
Circulodinium brevispinosum (Pocock 1962) Jansonius 1986
Circulodinium distinctum (Deflandre and Cookson 1955) Jansonius 1986
FAMILY CERATIACEAE
Muderongia brachialis Ottone and Pérez Loinaze 2002 Fig. 7K
Muderongia cf. *pariata* Duxbury 1983 Fig. 7B
Muderongia cf. *siciliana* Torricelli 1997
Muderongia spp.
Muderongia staurota Sarjeant 1966c
Phoberocysta neocomica (Gocht 1957) Millioud 1969 *emend.* Helby 1987 Fig. 7L
Pseudoceratium pelliferum Gocht 1957 *emend.* Dörhöfer y Davies 1980 Fig. 7J
Pseudoceratium sp.

Appendix C

Sample numbers, depths, number of particles or specimens counted per sample and palynofacies to which each sample belongs. SPM = sporomorphs, DINOCYST = dinoflagellate cysts, ACRTCH = acritarchs, PRASINO = prasinophytes, PALYNO = palynomorphs, FORAM = foraminiferal linings, TLHPhy = translucent lath-shaped phytoclasts, TLHBPhy = translucent biostructured phytoclasts, TEQPhy = translucent equidimensional phytoclasts, OLHPhy = opaque lath-shaped phytoclasts, OEQPhy = opaque equidimensional phytoclasts, AOM = amorphous organic matter, PFACIES = palynofacies.

Sample	Height	TETRAD*	SPM*	DINOCYST*	ACRTCH*	PRASINO*	PALYNO*	FORAM	TLHPhy	TLHBPhy	TEQPhy	OLHPhy	OEQPhy	AOM	GEL	SPM	DINOCYST	PRASINO	ACRTCH	Total	PFACIES
AG26a	485	10	139	0	0	0	149	0	143	3	112	64	142	0	4	18	0	0	0	486	1
AG23c	470	23	165	1	0	0	197	0	124	0	19	168	60	1	0	3	0	0	0	375	1
AG23b	464	25	141	1	0	0	170	0	120	0	32	156	44	0	1	10	0	0	0	363	1
AG23a	456	17	185	2	0	0	211	0	121	7	0	70	9	73	34	5	0	0	0	319	3
AG21a	444	29	166	11	0	0	213	0	286	0	0	141	51	4	0	23	3	0	0	508	1
AG20c	442	24	170	127	0	0	324	0	45	16	387	52	62	6	23	40	48	0	0	679	1
AG20B	431	5	126	25	0	0	167	0	64	0	55	112	45	6	7	30	3	0	0	322	4
AG19a	395	6	38	111	1	0	150	0	348	13	30	66	30	30	7	38	111	0	1	669	2
AG18T	389	1	54	96	0	0	150	0	288	0	0	143	49	28	27	37	49	0	0	621	2
AG18a	383	1	58	92	1	3	154	0	344	0	35	238	37	28	25	23	38	3	0	771	2
AG17a	375	1	57	93	0	0	151	0	5	0	0	180	184	4	0	5	1	0	0	379	2
AG15b	344	9	157	24	0	0	181	0	120	0	72	124	44	30	20	53	7	0	0	470	4
AG14c	317	6	109	50	0	0	159	0	48	0	17	104	51	14	4	45	17	0	0	300	4
AG14b	309	4	123	55	0	0	178	0	151	7	4	55	58	13	4	2	11	0	0	305	4
AG12b	281	1	43	15	0	0	58	0	58	0	29	191	97	28	6	2	2	0	0	433	2
AG12a	273	1	32	102	0	0	134	0	340	2	180	100	75	38	6	30	101	0	0	870	2
AG11b	245	1	61	9	0	0	72	0	60	4	825	20	22	17	6	17	1	0	0	964	2
AG11a	248	1	104	47	0	0	152	0	78	0	23	66	30	11	12	36	45	0	0	301	4
AG10d	246	2	137	18	0	0	156	0	73	0	12	128	59	1	36	6	4	0	0	300	4
AG10c	240	6	142	15	0	0	162	0	200	7	0	168	20	21	10	52	12	0	0	464	3
AG10b	236	6	107	47	2	0	154	0	119	0	70	120	45	18	5	12	5	0	0	400	4
AG10a	232	5	102	60	0	0	166	0	125	2	8	116	16	3	4	27	6	0	0	331	3
AG9b	218	6	149	17	0	0	172	0	108	0	10	340	39	4	12	23	8	0	0	538	3
AG9a	200	5	88	74	0	0	163	0	89	0	39	140	11	15	2	35	17	0	0	328	3
AG8b	199	3	197	43	0	0	236	0	232	16	44	196	67	15	0	62	3	0	0	638	4
AG.8a	197	7	152	3	0	0	156	0	235	0	35	111	25	2	2	23	8	0	0	447	4
AG7a	190	5	136	68	12	0	216	0	327	30	23	42	17	2	6	42	6	5	5	505	4
AG6b	187	1	152	15	0	0	168	0	229	0	17	358	42	26	2	26	1	0	0	675	3
AG6a	174	2	119	38	0	0	159	0	48	0	39	86	47	32	16	18	21	0	0	301	4
AG5b	170	1	54	112	0	0	166	0	117	1	14	143	19	57	13	46	1	0	0	453	3
AG5a	166	1	60	99	0	0	159	0	56	0	6	142	22	2	29	25	15	0	0	301	3
AG4b	160	2	105	64	0	0	171	5	91	2	7	161	7	22	0	10	43	0	0	312	3
AG4a	149	21	109	13	0	0	132	1	65	2	9	178	41	8	9	18	12	0	0	316	1
AG3d	143	3	66	101	0	0	168	11	72	5	3	47	5	127	3	17	36	0	0	315	5
AG3c	138	12	177	38	0	0	215	0	197	15	14	56	22	246	12	56	9	0	0	627	5
AG3b	134	10	246	21	2	0	269	0	203	4	0	165	15	65	0	24	4	1	0	481	3
AG3a	126	15	98	50	0	0	148	12	61	1	1	88	8	492	0	4	7	0	0	662	5
AG2b	118	4	130	40	0	0	177	0	163	7	13	371	32	4	2	52	7	0	0	651	3
AG2a	107	15	154	14	0	0	179	0	80	8	15	119	30	6	44	15	7	0	0	319	3
AG1c	99	3	98	66	0	0	164	0	39	2	1	509	107	25	8	8	7	0	0	706	3
AG1a	95	16	244	31	0	0	292	0	90	3	3	136	16	16	26	12	1	0	0	303	3
AG926	20	10	93	69	0	19	181	9	32	0	28	48	27	352	0	50	30	16	0	584	5
AM4	9	0	0	0	2	0	0	2	16	0	15	23	10	487	0	3	1	0	0	555	6
AM3	7	0	0	0	0	0	0	0	0	0	0	0	0	500	0	0	0	0	0	500	6
AM2	5	0	0	0	0	0	0	2	12	0	5	7	2	370	0	4	5	2	0	407	6
AM1	3	0	0	0	0	0	0	0	39	10	21	58	39	124	0	7	5	0	0	303	6
AM0	1	0	0	0	0	0	0	0	23	0	10	49	11	240	0	1	1	0	0	335	6

*Indicate categories of additional counting.